UNIVERSIDAD DE LA LAGUNA

BACHELOR THESIS

Anisotropy and Lifetime Decay of Green Fluorescent Protein in Glycerol

---

Author:
Maren Brauner

Supervisor:
Dr. Fernando Lahoz Zamarro

July 8, 2019

UNIVERSIDAD DE LA LAGUNA

Abstract

Science Faculty
Department of Physics

Bachelor Thesis

Anisotropy and Lifetime Decay of Green Fluorescent Protein in Glycerol

by Maren Brauner

Fluorescence is a phenomena that can be observed on the surface of tonic water in sunlight, perceiving the emission of blue light from a substance called *quinine*. In 1845 Sir John F. W. Herschel [1] discovered the previous phenomena. Nowadays, fluorescence embodies a useful research tool in various scientific fields such as biology, not only acting as a stain for diverse applications such as tracing cell organelles but also giving presumably important information about its environment such as the viscosity of the medium. This work is focused on the green fluorescent protein (GFP) with the objective to measure its emission spectra, its lifetime and anisotropy decay. According to the executed experiment, the result for the emission peak is, located in the green wavelength range at $\lambda_{em} = 510\,\text{nm}$. The lifetime decay also shows the expected behavior, involving the effects that occur during the excitation period. For the anisotropy decay measurements, the objective is to compare the measuring results with different models for the three dimensional shape of the GFP. Knowing a term called *rotational correlation time* θ from the experiment, the volume V of the protein can be determined. If the volume is defined and θ is measured, the viscosity of the medium that surrounds the GFP can be found. This part of the research was complicated as not all of the obtained data followed the expectations, hence, both models and ideas how to improve the procedure will be discussed theoretically in more detail.

Contents

Chapter 1

Introduction

Resumen

En la introducción se presenta, en primer lugar, la sustancia fluorescente principal de este trabajo: la proteína verde fluorescente (GFP). El primer apartado aporta una visión conjunta del fenómeno de la fluorescencia, del funcionamiento exacto de la transición de electrones a niveles energéticos más altos, así como de la desexcitación bajo emisión de fotones. También se explica el desplazamiento de la longitud de onda con respecto a la absorción en el espectro de emisión. Además, se nombra algunos mecanismos que pueden afectar a la propiedad fluorescente, como es el caso del "quenching", que tiene como consecuencia una disminución de la intensidad emitida. Finalmente se detalla la estructura y la maduración de la GFP, utilizando como punto de partida varios estudios y experiencias realizadas. Asimismo, se presentan los diferentes tipos de la proteína con los espectros correspondientes y sus aplicaciones conocidas en la biología celular, como la unión con orgánulos y proteínas celulares. Además se indican algunas ventajas de la GFP y varias aplicaciones interdisciplinarias.

The subsequent information is taken from the book *Principles of Fluorescence Spectroscopy* by Joseph R. Lakowicz [1] and the scientific articles [2] [3] [4] and [5], if no further mark is given.

1.1 Short explication of the Fluorescence Phenomena

In this chapter, the superordinate mechanism of fluorescence will be explained. It is known from atomic and quantum physics that radiating a substance with electromagnetic radiation can provoke an electronic transition. The typical

excitation for fluorescence means that one electron of the couple in the singlet ground state S_0 passes into a higher energy level of S_1. The instant disexcitation under light emission in less than 10^{-8} s [6], the so called fluorescence lifetime τ, is also characteristic for the phenomena.
The most outstanding fact is that the emitted light presents a longer wavelength than the excitation radiation, a discovery described for the first time by Sir George G. Stokes and therefore called *Stokes Shift*. The wavelength shift is connected to an energy loss during the electronic excitation due to internal conversions, where the transition of electrons to lower vibrational levels of S_0 and S_1 is caused by thermal energy liberation (non-radiative) shortly before or after the main radiative step from S_0 to S_1. The liberation of excess energy is also responsible for the independence of the emission wavelength from the excitation wavelength. Even if the electron is excited to higher vibrational levels of S_1, it mainly returns from the lowest level of S_1 to S_0 (Kasha's rule). During the excitation of the substance, some processes can affect the fluorescence. In the following a short definition of three of those processes will be given.

- **Quenching**: Destruction of the fluorescence caused by interaction (e. g. collision) with other molecules (quencher), but without destroying the fluorophore. The result is a decreasing fluorescence intensity.
- **Photobleaching [5]**: Permanent loss of fluorescence caused by radiation (e. g. a laser spot) that damages the fluorescent molecules. This phenomenon can be reversible, so the GFP can regain its fluorescence after a resting time.
- **Rotational Diffusion**: explained in 2.2.1

In this work, the considered fluorescent substance (fluorophore) is a protein, the Green Fluorescent Protein (GFP), presented in the next section.

1.2 Properties of Green Fluorescent Protein (GFP) and its advantages [7][8]

The Green Fluorescent Protein (GFP) is, as the name implies, a special green light emitting protein, showing a peak in the emission spectrum at 509 nm [9] (see figure 1.2). It is widely used in fluorescence spectroscopy, a tool for the analysis of a multifaceted number of substances by expressing the protein's

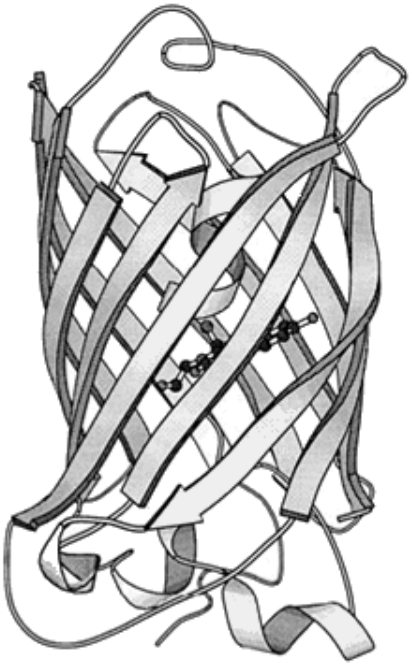

FIGURE 1.1: Tertiary structure of GFP [10], the residues forming an α-Helix responsible for the light emission in the interior and amino acid β-belts shaping a barrel

gene in the substance of interest. In the following, the advantages of the GFP in cell biology are going to be elaborated.
The protein, arising from the jellyfish *Aequorea victoria*, is composed of 238 amino acids. Their residues, the tripeptide sequences of Serine, Tyrosine and Glycine, provide the chromophore, the part of the protein responsible for light emission, in shape of an α-Helix in the tertiary protein structure. The remaining parts of the amino acids form a barrel of β-belts enclosing the chromophore as a protector, visible in figure 1.1.

At the beginning of the study of GFP, it was noticed that the jellyfish produces green light, a pretended contradiction to the fact that the involved protein *Aequorea* produces blue light. This problem was solved by finding out that the *Aequorea* only acts like an energy transmitter to excite the emission of green light by the actual GFP.
To allow the expression of GFP in systems beyond its natural appearance, the genetic information was extracted leading to a clone, the "apo-GFP", executed by Douglas Prasher. It became obvious that the characteristic fluorescence is independent of the system in which it is expressed, shown by the successful application in E.coli and C.elegans bacteria by Martin Chalfie. Later on, Roger Tsien determined that thitherto the unexplained maturation

of the fluorescence property in the primary structure of the tripeptide only oxygen is required and no further enzymes. The reaction with oxygen causes a deformation and builds up the desired fluorescence. Therefore, only the genes of Aequorea GFP are cloned, even if other types, such as *Obelia* from corals, exist, but these types need more complicated cofactors to mature than oxygen only.
Moreover, the GFP can be implemented to a living cell and its inferior structures, the organelles and internal proteins, with the purpose to visualize the movements within the cell and follow them during cell-typical processes, called protein targeting. In general, GFP is not toxic but it is supposed to liberate hydrogen peroxide during the chemical reactions of the maturing process which gives the GFP its final structure. Thus, a gain in the use of GFP is the fact that it does not change or destroy the components of the observed organism. This circumstance makes it suitable for being fused to a target and to substitute radioactive tracers.
The advantages of the GFP, aside from offering a high resolution in combination with imaging techniques, are the brightness of the fluorescent green light when excited by blue or ultraviolet light, the thereby connected photostability which means a high number of emitted photons, the simplicity to form a bond with proteins of interest and the rapid folding and maturing of the chromophore.

1.2.1 Classification and further applications of GFP

Based on the chromophore components, different classes show various emission bands within the visible spectrum, to be more precise, the distinction lies in the produced peaks, of which some are shown in figure 1.2. The succession starts with class 1, the wild type, and ends with class 7 in descent wavelength bands. The classes can provide improved characteristics, like an enhanced brightness, and may be more appropriate for certain applications [11]. The different classes and the corresponding mutants are listed in [7] on page 519.

As mentioned before, the types of GFP and its improved versions, the mutants, depending on the required properties, are used as a tag, which means the fusion to other proteins or organelles of a cell to follow their motion.

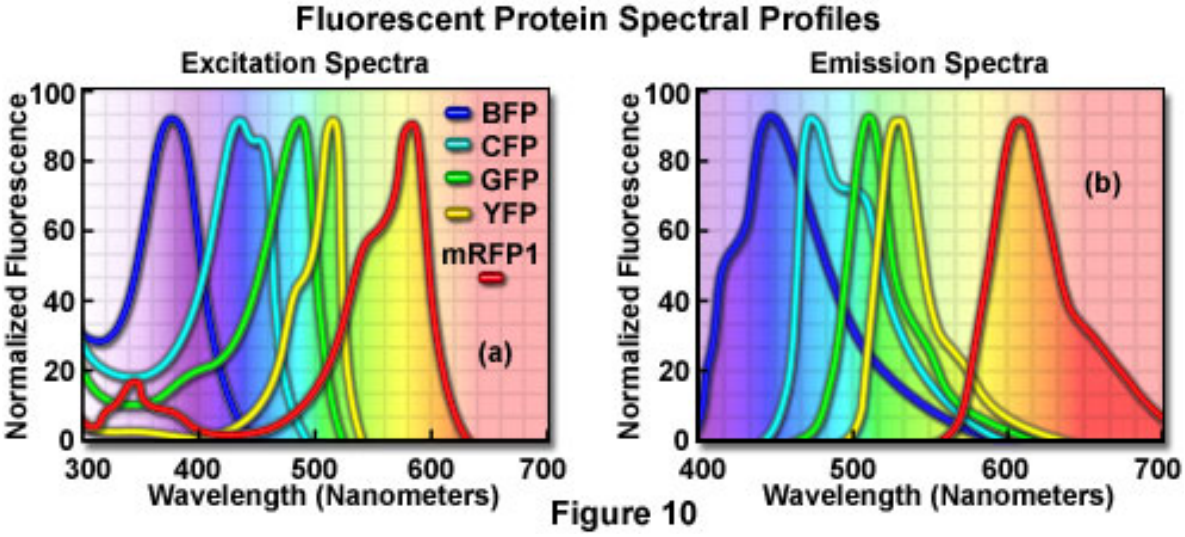

FIGURE 1.2: Excitation and Emission spectra of GFP mutants, with the emission colors blue (BFP), cyan (CFP), yellow (YFP), red (mRFP1) and the original green GFP [12] [1]

Furthermore, it serves as an indicator influenced by the change of its fluorescence caused by reactions with its environment, for example to detect the fluidity of membranes or the viscosity of cytoplasm, the main topic of this work.

In summary, the GFP turns out to be a universal tool in the mentioned scientific field of cell biology. The next step is the development of mutants [2], to amplify the application possibilities and create new methods such as sensors of Ca^{2+} and other substance concentrations in organisms.

Other interesting and also interdisciplinary application areas are for example medical diagnosis, forensic and genetic analysis [1]. A concrete example is the tracing of the influenza virus and the corresponding inhibitors deriving from drugs [13].

Chapter 2

Theoretical background

Resumen

El segundo capítulo comienza con una delimitación terminológica de las expresiones físicas utilizadas con la presentación de sus expresiones analíticas. Para ello se define, en primer lugar, el término del tiempo de vida τ y su desintegración con el tiempo. Seguidamente, se explica la polarización P y el término equivalente de la anisotropía r en el régimen permanente y dependiente del tiempo. Esto incluye mencionar que la anisotropía también obedece a la ley de la desintegración, las distribuciones de las intensidades y los detalles de la conservación del momento de transición. Otro concepto importante es el "rotational correlation time θ", es decir, el tiempo necesario para el giro de un radián de la proteína, un factor que cambia la orientación de los momentos de transición y por lo tanto, la polarización de la emisión. El valor de θ es útil para la determinación de la viscosidad del entorno de la proteína cuando se conoce el volumen de la GFP y viceversa.

The following theoretical facts are taken from the book *Principles of Fluorescence Spectroscopy* by Joseph R. Lakowicz [1], if no further mark is given.

2.1 Fluorescence Lifetime

The already mentioned fluorescence lifetime τ describes the time between excitation and disexcitation of the fluorophore and therefore the time range for possible interactions which change the nature of the emission. In this work, the considered interactions take place between the GFP and the used solvent glycerol in different concentrations.
The electrons do not remain in the excited state for the same time, in such a way that the value of τ is the average over the individual lifetime of every

electron.
The time development of fluorescence intensity, which is proportional to the number $n(t)$ of excited molecules [14], follows the familiar decay law

$$I(t) = I_0 e^{-\frac{t}{\tau}} \tag{2.1}$$

with initial intensity I_0 and lifetime τ. The lifetime can be influenced by the refractive index of the environment, the fluorophore concentration and other molecules that act like quenchers [15].

2.2 Fluorescence Anisotropy in the steady state

The general definition of anisotropy is the directional dependence of any physical magnitude. In fluorescence anisotropy, the emitted light presents a special direction or polarization. The term anisotropy means the extent of polarization in the emission. For this reason, fluorescence anisotropy r and fluorescence polarization P can be used to describe the phenomena and the mathematical expressions for r and P can be transformed into each other.
The excitation light providing from a laser is vertically polarized and the explanation for polarization of the emitted light lies in the distribution of transition (dipole) moments in the sample [16]. The transition moment provides a proportion of the ability of a molecule to absorb or emit radiation. It is a vector quantity, and in homogeneous solutions it has an isotropic orientation. The transition moments of a molecule which are oriented parallel to the direction of the electric field of the incident light, are excited most likely what is called *photoselection*.
Since the excited state preserves the orientation of the transition moment in many cases, the majority of the transition moments in excitation are also vertically oriented. As a result, the liberated radiation in the disexcitation shows the same polarization as the excitation light.
However, there is also the possibility, that the transition moments change their orientation (see 2.2.1) and the emission polarization is not completely parallel to the excitation, thence the total emission intensity I_T has two parts: $I_{\parallel}$ parallel to the polarization of the incident light and $I_{\perp}$ perpendicular to it. The anisotropy as the extent of polarization is now defined as the normalized difference between the two components

$$r = \frac{I_{\parallel} - I_{\perp}}{I_x + I_y + I_z} = \frac{I_{\parallel} - I_{\perp}}{I_{\parallel} + 2I_{\perp}} \tag{2.2}$$

with the total intensity $I_T = I_x + I_y + I_z$ as the sum of the intensities in every cartesian direction. The total intensity for normalization

$$I_x + I_y + I_z = I_{\parallel} + 2I_{\perp} \tag{2.3}$$

is derived from the consideration that the incident light is polarized in the z-direction and the remaining parts I_x and I_y are distributed symmetrically around the z-axis and therefore contribute to $I_{\perp}$ in the same amount, even if the x-direction also describes the direction of light propagation.
In contrast to the anisotropy, the polarization does not count the intensity I_x as a part of $I_{\perp}$. The expression for the polarization P is:

$$P = \frac{I_{\parallel} - I_{\perp}}{I_{\parallel} + I_{\perp}}. \tag{2.4}$$

Using simple transformation formulas, P and r can be transformed into each other. Both expressions contain the same information, although not being equal. Nevertheless r is more frequently used.
A graphic explanation for the outlined polarization measurements can be found in figure 2.1.

As the formulas indicate, the limit cases of r and P are the complete polarization, only observable in fully orientated samples, it means that $I_{\perp} = 0$ and $P = r = 1$ and completely unpolarized (isotropic) samples $I_{\parallel} = I_{\perp}$ which leads to $P = r = 0$.
If the laser radiation is constant, which is equal to the steady-state, the anisotropy r from equation 2.2 can only give an average of the anisotropy.

2.2.1 Rotational Correlation Time and Anisotropy Decay

Leaving the steady-state, time dependent values of r obtained by pulsed excitation can be used to estimate the shape, size and flexibility of the molecule in question.
In the case of a spherical molecule the anisotropy decay can be detected by measuring the decays of the parallel and perpendicular components of the emitted light after the excitation with a vertically polarized pulse. The anisotropy decay can be expressed by making use of equation 2.2 respecting that the intensities and r itself are time dependent (later introduced in formula 3.1). The time-dependent anisotropy decay $r(t)$ is independent of the lifetime τ. In fact, the lifetime supplies the limits of the intensity measurements or rather the time range of the decay.

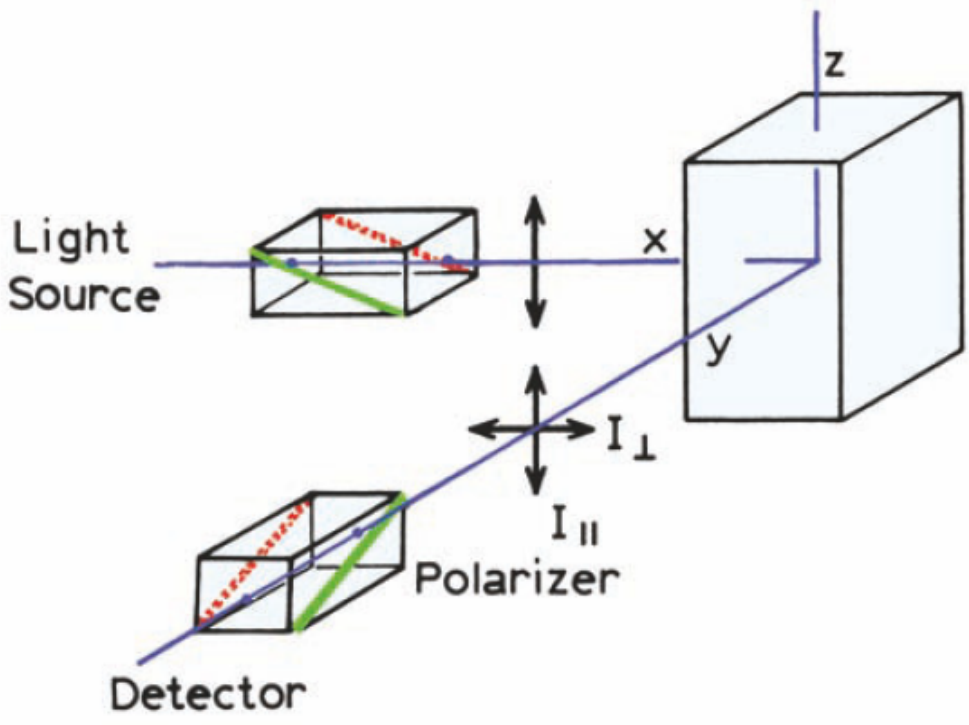

FIGURE 2.1: Diagram for measurement of fluorescence polarization (page 354)[1] and a simplified schema of the functionality of the spectrofluorometer (see chapter 3) in anisotropy experiments

Another expression for the anisotropy decay of a spherical molecule showing more simplicity and also belonging to the time-domain anisotropy measurements is

$$r(t) = r_0 e^{-\frac{t}{\theta}} \tag{2.5}$$

with the initial anisotropy without rotational diffusion r_0, and the rotational correlation time θ. Supposing that the initial anisotropy r_0 is given by[1]

$$r_0 = \frac{2}{5}\left(\frac{3\cos^2(\beta) - 1}{2}\right) \tag{2.6}$$

also called intrinsic displacement of the excitation and emission transition moments without other effects that change the polarization, with β as the displacement angle between the absorption and emission dipoles. For $\beta = 0°$, the intrinsic displacement reaches its maximum of $r(t = 0) = 0.4$, but in practice $r_0 < 0.4$.

During the short excitation stage, it is possible that the fluorophore changes

the orientation of its transition moments by a rotational motion called *rotational diffusion*, describing the displacement of the transition moments changing the polarization of the emission. The rotational diffusion can be expressed by the term of rotation correlation time θ which affords the average time it takes for a molecule to rotate by one radian. It depends on the size and the shape of a molecule and furthermore on the viscosity of the solution. Its analytic expression depends on the volume of the molecule, the environmental temperature and the viscosity (see chapter 4 equation 4.7). In highly viscose solutions it might occur that θ becomes very large because of the drag in viscosity, consequently, the rotation stops and the orientation of transition moments cannot change. In contrast, in low viscosity solutions with small fluorophores the rotational diffusion is higher than the emission rate, so the orientation can change during the excitation state and the emission becomes depolarized. In this case the anisotropy 2.5 is close to zero. The result is that the measurement of r permits to study the angular displacement in the excitation stage.

For a spherical molecule, one of the models for the GFP (see chapter 4) only one rotational axis is expected, leading to a single rotational correlation time θ (equation 2.5). In practice $r(t)$ consists of more than one exponential because more complex molecules (e. g. some proteins) can have more than one rotational axis. Therefore, determining the rotation correlation time helps to find the shape of these molecules.

If parts of the molecule rotate individually, seen by obtaining very short correlation times, too short for the motion of the whole molecule, the characteristic of segmental flexibility becomes visible.

To close this theoretical chapter and translating these facts to the subject of this work, it can be said that knowing the exact shape of the molecule, in this case the GFP, anisotropy decay measurements, in particular determining the rotational correlation time, lead to find the viscosity of the medium that surrounds the protein, explained with more detail in chapter 4.

Chapter 3

Experimental Research

Resumen

En este capítulo se describe la configuración experimental, consistente principalmente en un láser diódico, un instrumento de espectroscopia especial para medidas de fluorescencia, el LifeSepc II, y un detector conectado con un ordenador provisto con un programa de análisis de datos.
Además, se explica el método experimental, es decir, la determinación previa del factor de corrección G y su origen, las medidas del espectro de emisión, del tiempo de vida y la anisotropía fluorescente, añadiendo glicerina a la mezcla inicial de agua-GFP y observando el desarrollo de los datos de cada parte con la concentración de glicerina.

3.1 Instruments and Measuring Configuration[17]

The most important instrument for this research is the so called spectrofluorometer of the type LifeSpec II from Edinburgh Instruments [17] which allows besides the spectra analysis, lifetime measurements and anisotropy decay with great accuracy. Figure 3.1 shows the interior of the measuring device. The beam, provided by the excitation source, in this case a picosecond pulsed diode laser (EPL Series) of the wavelength 470 nm also from Edinburgh Instruments, is reflected by a mirror and passes through an attenuator to control the intensity of the beam before entering the sample chamber. At this point, the beam's natural vertical polarization can be improved by using a polarizer. The laser excites the sample in the chamber and the emitted light goes through a 495 nm low-pass filter to exclude the laser light from detection, and passes the emission polarizer (analyzer) eventually. Afterwards, it enters the monochromator and, for isolating the wavelengths, a shutter is

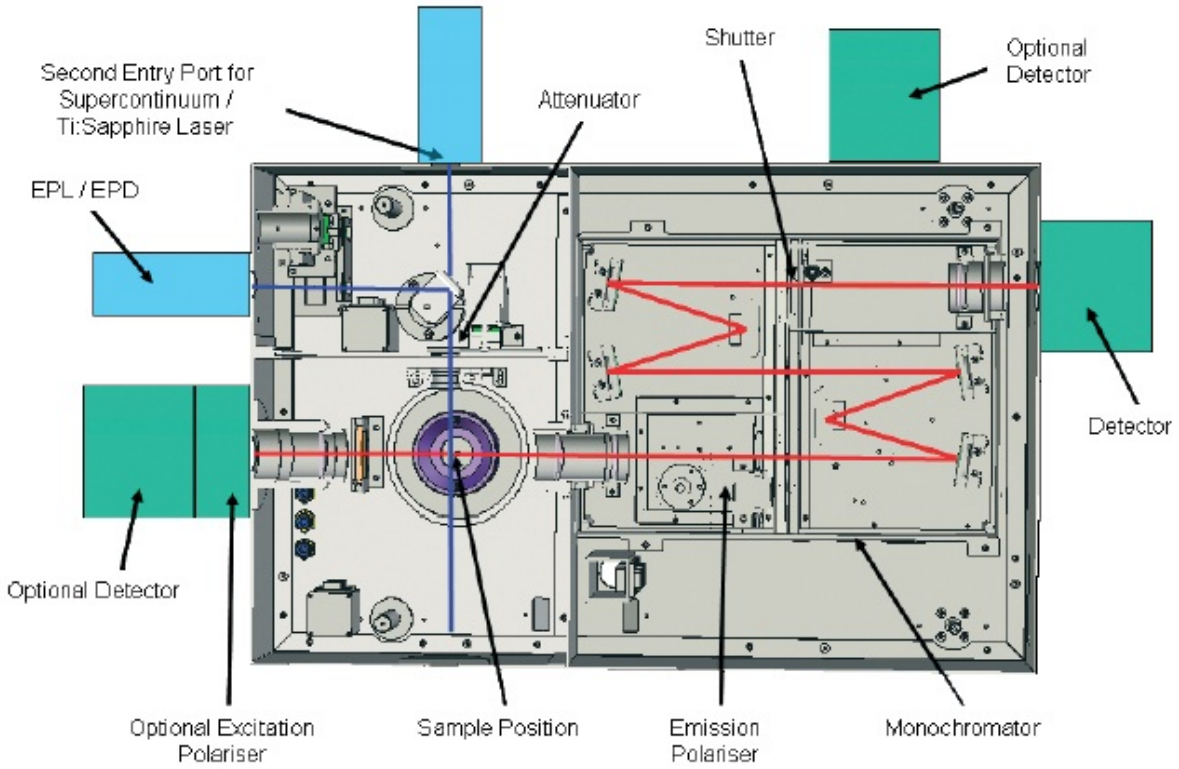

FIGURE 3.1: Spectrofluorometer LifeSpec II [17], only the EPL source and the detector on the right have been used, the polarizer for the excitation beam and the 495 nm filter is missing in the layout

placed in front of the detector. Finally, a computer processes the data received from the detector. Due to the fact that only one detection system was used, thereupon the vertical and horizontal components of the emission are measured successively via the same channel, the method is called Single-Channel Method [1]. To guarantee a focused beam during the passage, it is possible that the device contains additional optical components such as lenses [1]. It is also possible to cool down the sample by introducing a coolant to the sample chamber. This detail could be of interest for the improvement of the experimental procedure (see chapter 4).

The associated software F900 has been used to analyze not only the spectrometer setup and controlling but also the data processing and imaging.

The final graphical analysis (see chapter 3) was executed via the data analyzing tool Origin 7.0 from OriginLab.

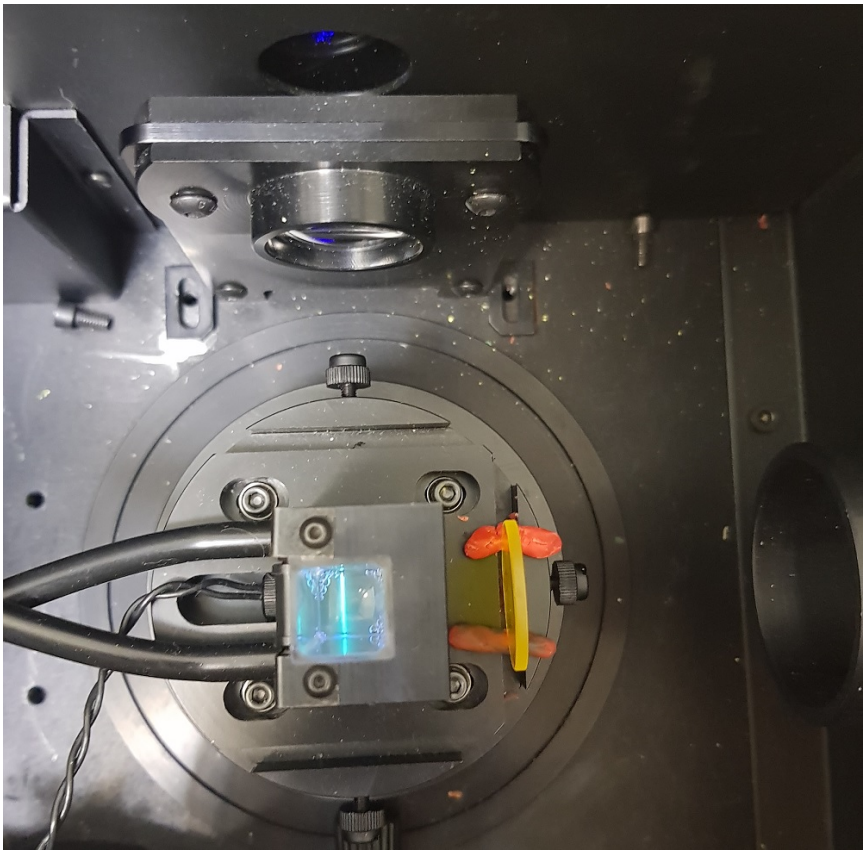

FIGURE 3.2: Image of the sample chamber, the blue laser beam from the top and the yellow filter between the cuvette and the entrance to the monochromator can be seen. In this case the sample is the pure water-GFP mixture, the unattenuated fluorescence green light emission is clearly visible

3.2 Methodology

Inside the sample chamber, a cuvette containing the probe was placed in a support in the path of the beam. The starting point of the experiment is a sample of GFP solved in water. By placing the cuvette in the sample position, the light emission became visible, captured in Figure 3.2. After checking the right transmission of the beam through the sample and controlling the beam intensity to avoid damage of the detector, the measures of the emission spectrum, the fluorescence lifetime and the anisotropy decay have been initialized. The single procedures are presented with more detail in the following paragraphs.

Emission Spectrum For the emission spectrum, the emitted wavelengths are sampled in steps of 1 nm by the monochromator and the corresponding intensities to the wavelength fractions are detected for 0.5 s (dwell time).

Fluorescence Lifetime The lifetime, so the time between excitation pulse and photon emission, is measured by adjusting the monochromator near the emission peak from the previous step, in this case 510 nm, and detecting the intensity for 200 s in a lifetime range of 50 ns. A short pulsed excitation leads to the emission and detection of only one photon, called Time-Correlated Single Photon Counting (TCSPC) [18]. The detected lifetimes are summarized in a histogram, illustrating the distribution.

Anisotropy Decay The measurement procedure of the anisotropy decay, the procedure is similar to the one of the lifetime, however, the main difference is that the detection polarizer is used, measuring $I_{\parallel}(t)$ and $I_{\perp}(t)$ to apply equation 2.2 in the time dependent version

$$r(t) = \frac{I_{\parallel}(t) - I_{\perp}(t)}{I_{\parallel}(t) + 2I_{\perp}(t)}. \tag{3.1}$$

The data analyzing software calculates $r(t)$ out of $I_{\parallel}(t)$ and $I_{\perp}(t)$ for the time range 50 ns.

The emission spectrum is recorded by a steady state measurement, a constant radiation of the probe, and the decay measurements are part of time resolved spectroscopy, summiting the probe to light pulses shorter than the fluorescence lifetime, thus the disexcitation can be measured without reaching the steady state immediately [1].
The three measurements were repeated after adding glycerol $C_3H_8O_3$, a trihydroxy sugar alcohol, to the water-GFP mixture. Doing so, the glycerol concentration increased successively from 0 % to approximately 82 %.
It has to be mentioned that the results for the emission spectrum and the fluorescence lifetime originate from a different sample than the anisotropy decay results, as the anisotropy measurements have been repeated in a second session with the intention to improve the results (see chapter 4).
Furthermore, like already brought up, the correction factor for the monochromator, called G-factor has to be determined [1]. The efficiency of the monochromator is not the same for the two adjustment possibilities, parallel and perpendicular to the excitation polarization. The G-factor is defined as the sensibility ratio of the monochromator of the vertical and the horizontal intensity

components of the emission, responsible for the fact that the executed intensity measurements I_{VV} (vertical excitation, vertical emission) and I_{VH} (vertical excitation, horizontal emission) differ from the real intensities $I_{\parallel}$ and $I_{\perp}$:

$$\frac{I_{VV}}{I_{VH}} = G\frac{I_{\parallel}}{I_{\perp}}. \tag{3.2}$$

In practice, the G-factor can be measured by rotating the laser into the position that it provides a horizontal polarized beam, so that transition moments lying in the xy-plane are excited. Because of symmetry, the two directions are excited to the same extend and the detected intensities $I_{\parallel}$ and $I_{\perp}$ (right side of 3.2) must be the same. In reality, however, the measured values I_{HV} and I_{HH} are not the same and their ratio is not equal to one as expected, but knowing

$$\frac{I_{HV}}{I_{HH}} = G\frac{I_{\perp}}{I_{\perp}} = G, \tag{3.3}$$

the measurement of I_{HV} and I_{HH} leads to the determination of G. It is the previous step of every experimental session as G affects the anisotropy in the following way:

$$r = \frac{I_{VV} - GI_{VH}}{I_{VV} + 2GI_{VH}}. \tag{3.4}$$

The obtained value for G is introduced to the anisotropy measurement control section of the program so that the obtained anisotropy results are already corrected. Essentially, the G-factor was determined only in the first two sessions to be 0.38 and 0.40, and later on fixed as 0.40.

Chapter 4

Measuring results and discussion

Resumen

A continuación se presentan los resultados de las tres partes del experimento. Se puede verificar que el espectro de emisión medido coincide con las expectativas y que la media de los resultados de cada concentración se desvía con un porcentaje pequeño del valor teórico de $\lambda_{em,th} = 509\,\mathrm{nm}$. *Además, se explica de forma razonada por qué el espectro tiene la forma de una distribución y se indica el efecto del ruido a concentraciones altas, una observación importante también para las otras partes. Posteriormente, en la parte del tiempo de vida se aportan resultados de los ajustes y una ampliación de las expresiones teóricas. Una de estas expresiones es la ecuación conocida como formula de Strickler Berg, que es utilizada para evaluar los resultados obtenidos. Por último, la desintegración de la anisotropía no muestra el comportamiento esperado y se discute los posibles fuentes de errores, como la dispersión de los fotones. Para ello se indica el procedimiento alternativo del ajuste, explicando la problemática ocurrida con detalle. Finalmente, se presenta las expectativas para los resultados en el caso de la anisotropía, basándose en distintos modelos de la forma hidrodinámica de la GFP, como una esfera o directamente su forma cilíndrica.*

4.1 Results

4.1.1 Emission spectra

The emission spectrum of GFP in an increasing glycerol concentration is presented in figure 4.1. The first observation is that the emission spectrum is not altered by the glycerol. It turns out that the measured wavelength maxima, summed up in table 4.1, are located around the theoretical emission wavelength $\lambda_{em,th} = 509\,\mathrm{nm}$ [9] with an average value of $\lambda_{em} = 510\,\mathrm{nm}$. Thus, the relative deviation of the average is about 0.20 %, so the result reflects the

expectation.
The reason to the question why the emission spectrum has the shape of a distribution rather than showing a sharp peak at $\lambda_{em,th} = 509\,\text{nm}$ is similar to the explication of the question why several wavelengths can be absorbed: as the molecule can be excited to different levels of S_1 (see 1.1), it can also emit photons with different energies, returning to various levels of S_0, because of subsequent internal conversions. The maximum in the recorded spectrum belongs to the level of S_0 which is reached with the utmost probability.

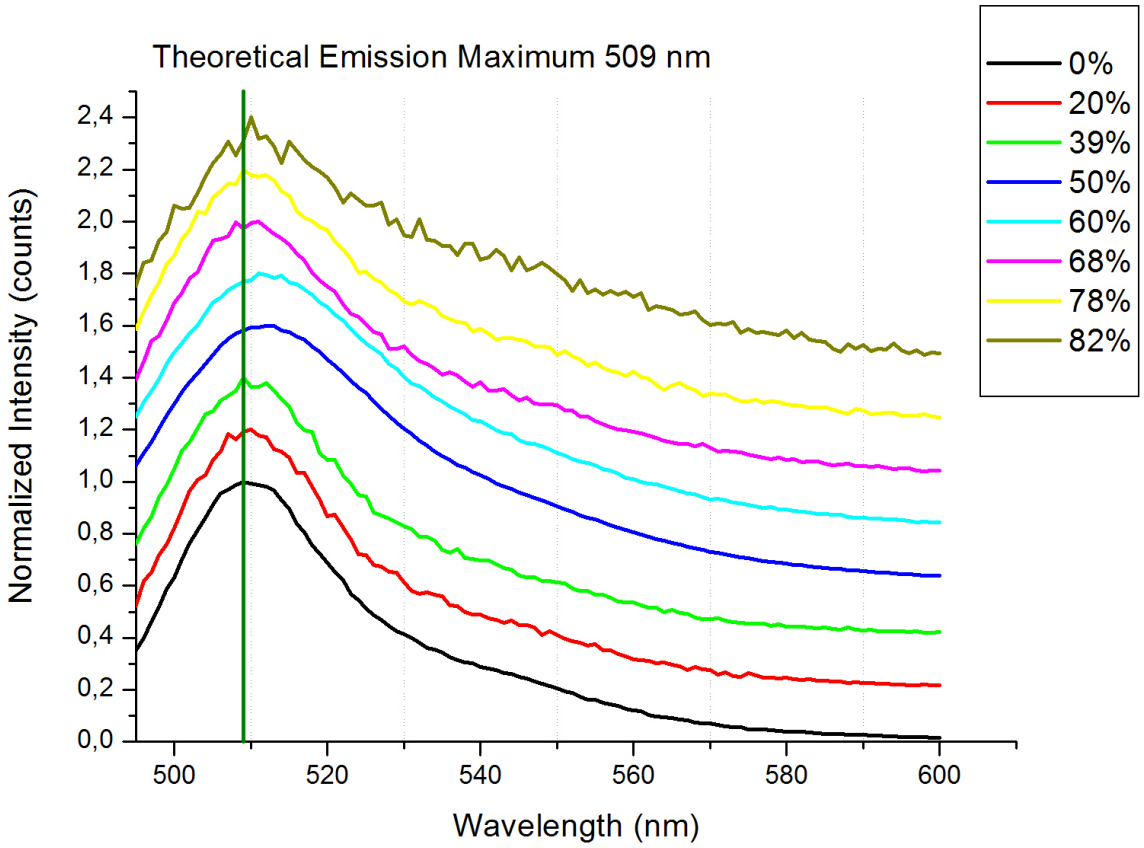

FIGURE 4.1: Normalized Emission curves for the studied concentrations of glycerol. The curves present an intensity offset of 0.2 relative to each other. The vertical line shows the position of the theoretical emission maximum [9]

The curves of the highest concentrations, especially the one of 82 % glycerol, is less smooth than the others, however containing more random noise which is an important observation regarding the following paragraphs. It may be connected to the decreasing concentration of GFP and therefore decreasing intensity of the emission that makes the measurements more vulnerable to random noise (scattering, later explained with more detail).
In addition, the curves of 50 %-68 % are smoother because of an elevated

number of counts per second (cps), higher than in the case of the other concentrations but less than the number of cps that can cause damage to the detector. The high number of cps originates from the iris setting that controls the intensity of the laser beam, which was higher than it should have been in these three measurements.

TABLE 4.1: Emission maxima extracted from figure 4.1. The resulting average is $\lambda_{em} = 510\,\text{nm}$

Concentration [%]	Wavelength λ_{max} [nm]
0	509
20	510
39	509
50	512
60	511
68	511
78	509
82	510

4.1.2 Fluorescence lifetime decay

The lifetime decay results can be found in figures 4.2-4.4. The logarithmic scale was used because it illustrates the difference of the concentrations more than the normal scale. In addition, the combination of 60 % and 82 % in 4.4 was chosen due to the fact that the concentration values are more separated than 60 % and 68 %. The plot combination of 60 % and 68 % is added in the appendix A as figure A.1.
The fit function for the exponential fit has the form of the decay law

$$I(t) = I_0 e^{-\frac{t}{\tau}} + y_0 \tag{4.1}$$

just as indicated in equation 2.1 with the parameter y_0 to have more flexibility in fitting the curve. Following the equation 2.1, $y_0 \approx 0$ and $I_0 \approx 1$ as the data was normalized before the fitting. These criteria for the parameters were satisfied in each case.
The obtained lifetimes, with the corresponding errors and the coefficients of determination calculated by the fitting program, are summed up in table 4.2 and also visualized in figure 4.5 to point out the development of τ with the concentration. The fitting algorithm used by Origin 7.0 is the Chi-Square

Minimization and the errors of the derived parameters are obtained by the error propagation formula (see manual of Origin 7.0).

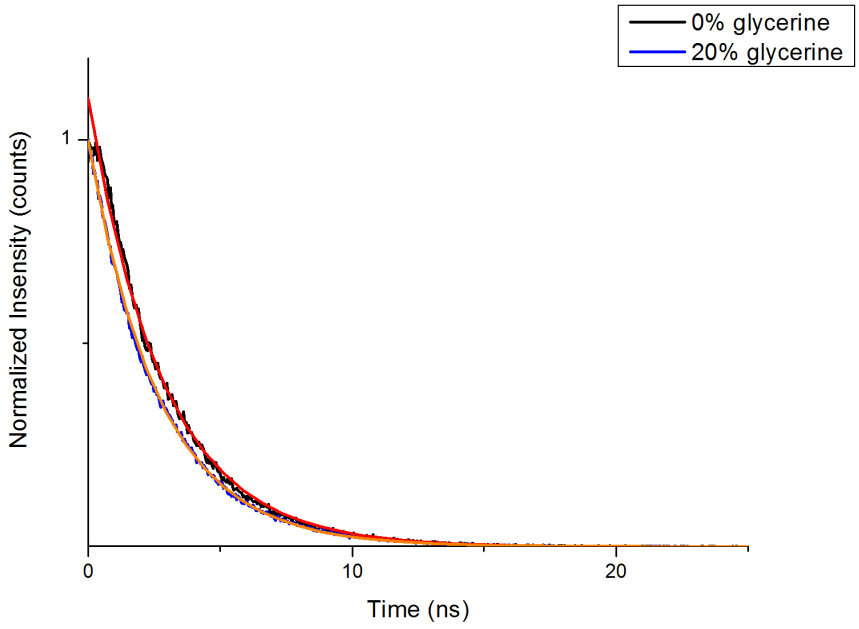

FIGURE 4.2: Fluorescence lifetime decay of 0 % and 20 % glycerol solvents. Normal scale. The lifetime values are $\tau_0 = 2.84 \pm 0.01$ ns and $\tau_{20} = 2.673 \pm 0.004$ ns, coefficients of determination $R_0^2 \approx 1$ and $R_{20}^2 = \approx 1$

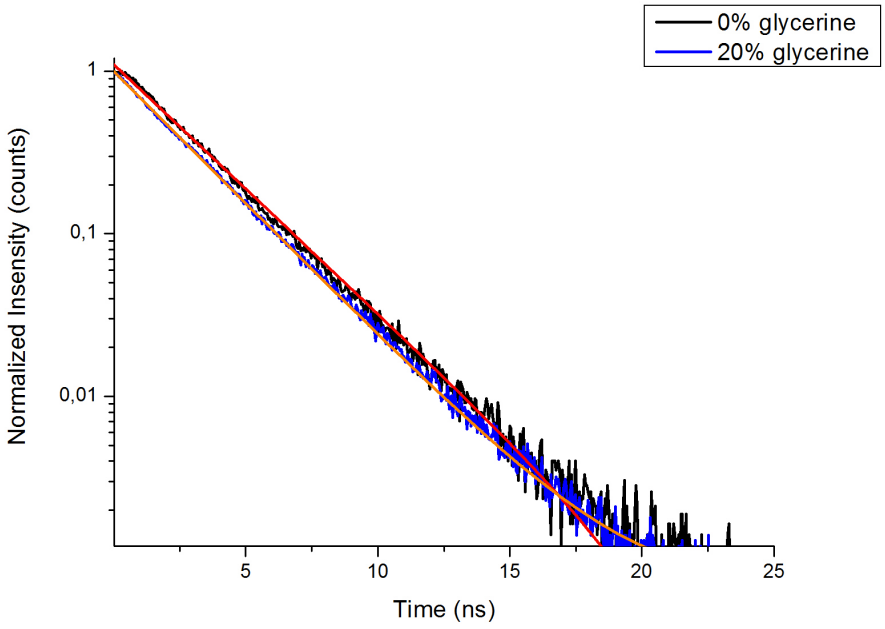

FIGURE 4.2: Fluorescence lifetime decay of 0 % and 20 % glycerol solvents. Logarithmic scale.

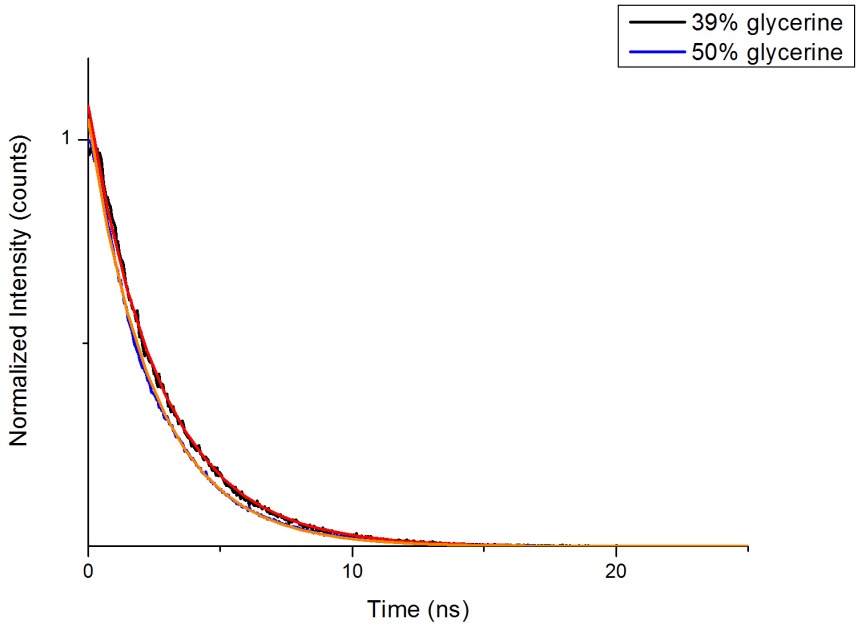

FIGURE 4.3: Fluorescence lifetime decay of 39 % and 50 % glycerol solvents. Normal scale. The lifetime values are $\tau_{39} = 2.747 \pm 0.008$ ns and $\tau_{50} = 2.472 \pm 0.004$ ns, coefficients of determination $R^2_{39} \approx 1$ and $R^2_{50} \approx 1$

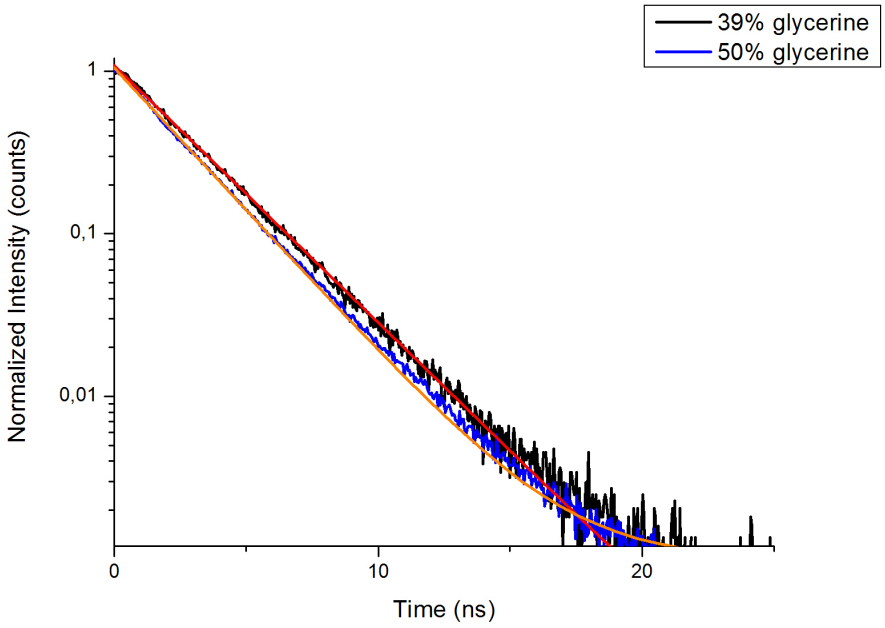

FIGURE 4.3: Fluorescence lifetime decay of 39 % and 50 % glycerol solvents. Logarithmic scale.

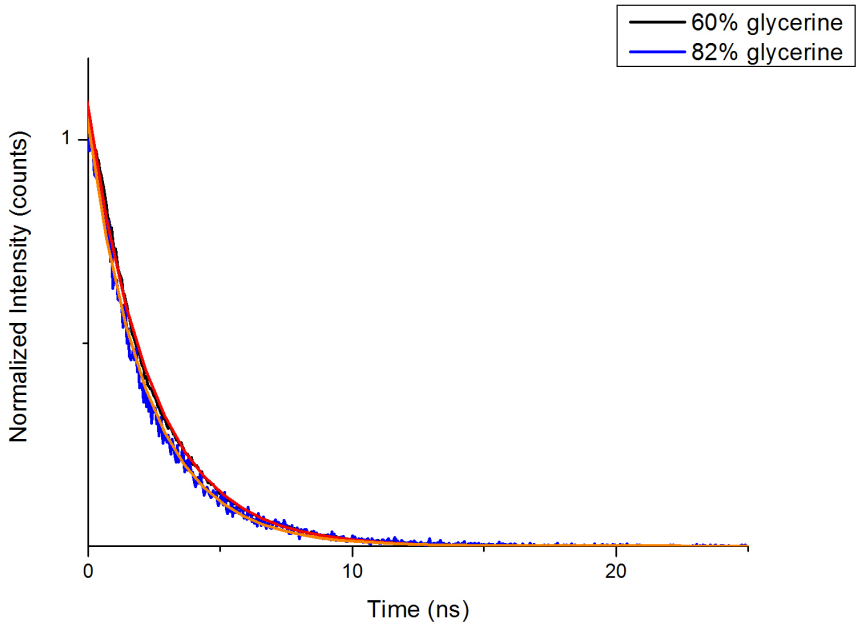

FIGURE 4.4: Fluorescence lifetime decay of 60 % and 82 % glycerol solvents. Normal scale. The lifetime values are $\tau_{60} = 2.401 \pm 0.007$ ns and $\tau_{82} = 2.221 \pm 0.009$ ns, coefficients of determination $R^2_{60} \approx 1$ and $R^2_{82} \approx 1$

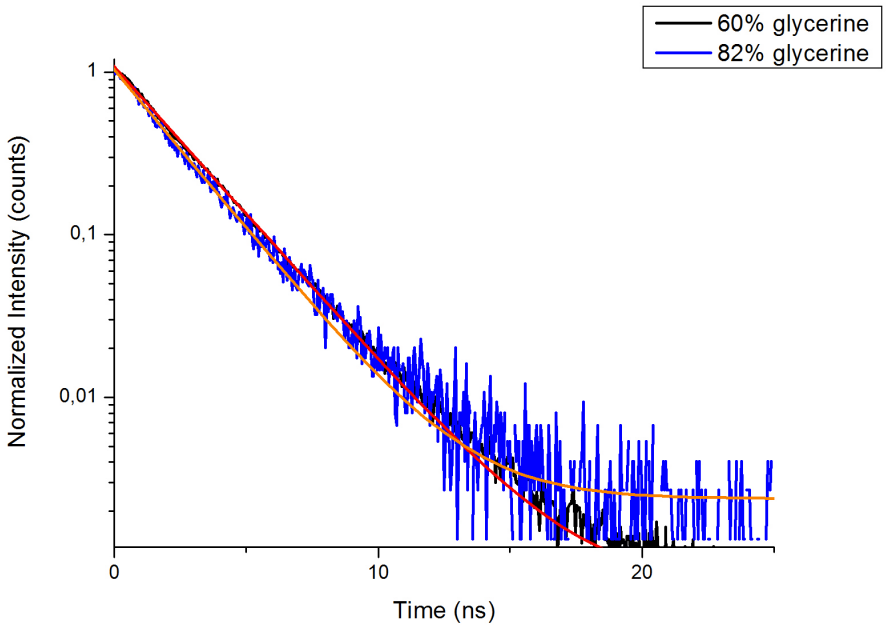

FIGURE 4.4: Fluorescence lifetime decay of 60 % and 82 % glycerol solvents. Logarithmic scale.

Analyzing the parameter and the coefficients of determination, which are

close to 1, means that the data matches with the fitting function, therefore it can be suggested that the curves show the expected decay behavior of 2.1.
As in the previous section, the random noise increases with the concentration of glycerol, in particular, it becomes visible for 82 % glycerol. For higher concentrations of glycerol and thus a lower concentration of GFP, the higher number of glycerol molecules ascertain more possibilities for deviating the light emissions. With a lower concentration of GFP, less proteins are excited because the laser beam only reaches a lower number of GFP. As a result, the intensity decreases and the random noise grows.
Another important point is the fact that the lifetime decreases with an increasing concentration as indicated in figure 4.5. Further research on the explanation of this observation shows that the theoretic expressions given in 2.1 needs to be amplified. Like elaborated before, the depopulation processes of the excited state belongs to two different types: the radiative and the non-radiative type. The rates of the conversions are called k_r for radiative and k_{nr} for non-radiative conversion [19] [1]. Now the inverse of the lifetime is the sum of these two rates [19]

$$\frac{1}{\tau} = k_r + k_{nr}. \tag{4.2}$$

and in general $k_r > k_{nr}$ [1]. The part of the lifetime caused by radiation τ_0 is named natural radiative lifetime

$$\frac{1}{\tau_0} = k_r. \tag{4.3}$$

A formula, the Strickler Berg formula, relates the natural radiative lifetime with the emission spectra $I(\bar{\nu})$, an extinction coefficient ϵ and the refractive index n [19] [20]

$$\frac{1}{\tau_0} = k_r = 2.88 \cdot 10^{-9} n^2 \frac{\int I(\bar{\nu}) d\bar{\nu}}{\int I(\bar{\nu}) \bar{\nu}^3 d\bar{\nu}} \int \frac{\epsilon(\bar{\nu})}{\bar{\nu}} d\bar{\nu}. \tag{4.4}$$

As the emission does not change with the increasing glycerol concentration, the interesting fact extracted from the formula is

$$\frac{1}{\tau_0} = k_r \propto n^2. \tag{4.5}$$

and therefore $\tau^{-1} \propto n^2$. The values for the refractive index can be found in table [21]. A graphic plot showing the expected linearity is presented in figure 4.6. The curve can be compared to figure 4 from [22]. Only the inverse lifetime value of 0 % includes the fitting line in its error interval, the other

TABLE 4.2: Lifetime results summed up

Concentration [%]	Lifetime [ns]
0	2.82 ± 0.01
20	2.673 ± 0.004
39	2.747 ± 0.008
50	2.472 ± 0.004
60	2.401 ± 0.007
68	2.417 ± 0.008
82	2.221 ± 0.009

lifetimes are close to the line, except the outlier value of 39 %. So the general trend, given by the Strickler Berg equation, is followed by the measured lifetime results.

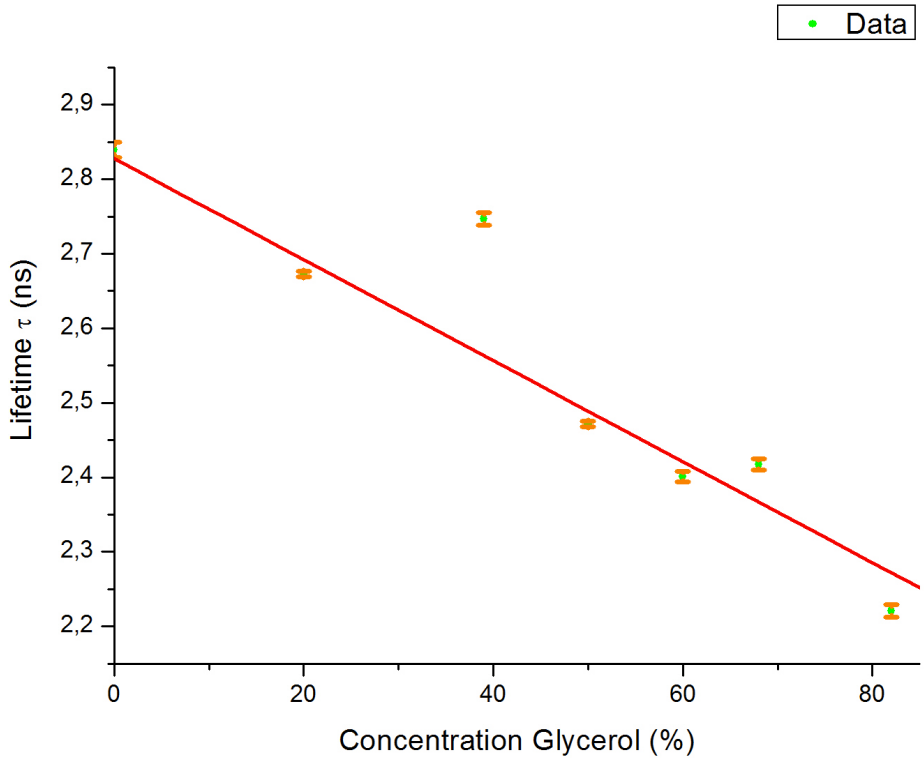

FIGURE 4.5: Development of the lifetime τ with increasing glycerol concentration

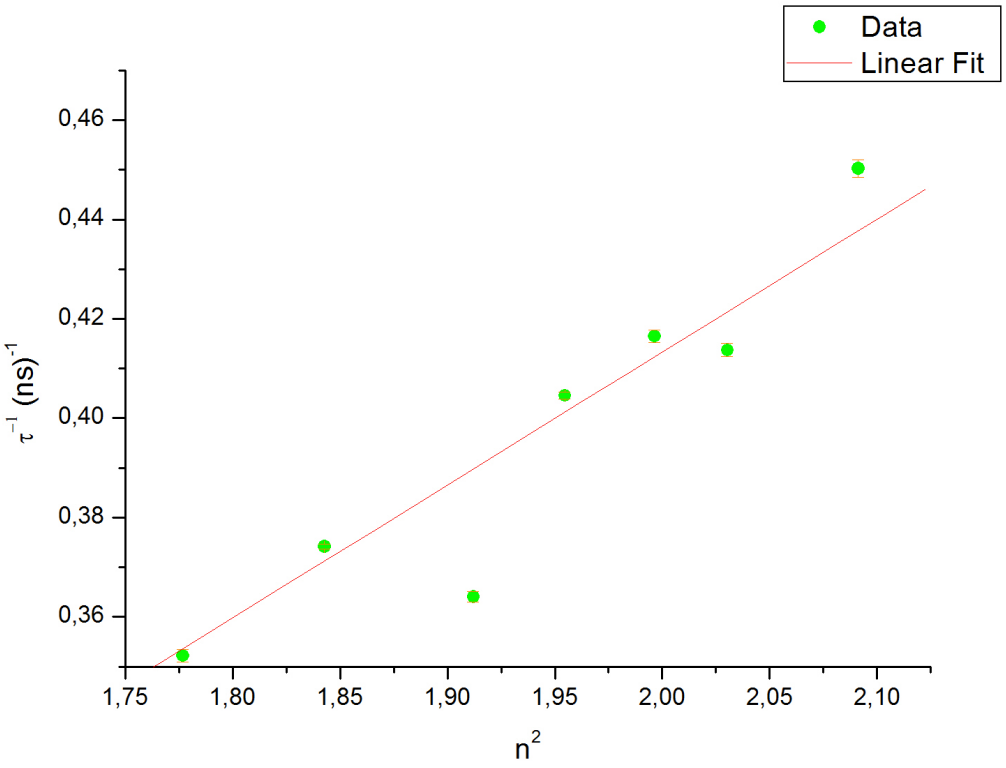

FIGURE 4.6: Fluorescence lifetime from 4.2 plotted versus the refractive index squared n^2 [21]

4.1.3 Anisotropy decay

The anisotropy decay results for the concentrations of 0 % and 20 % are presented in figures 4.7 and 4.8. The data was not time shifted, meaning that the decay does not start at time zero, because the shift would have changed the results of the fit. Instead, it was possible to see, that the decay data starts at about 5.9 ns, which was the first fixed limit of the fitting range. In the next step, it was necessary to approximate where the data descends to noise and find the second limit of the range. This part was complicated, since the parameters showed great fluctuations, for that reason it was tried to amplify the range in small steps and execute the fitting with

$$r(t) = r_0 e^{-\frac{t}{\theta}} + y_0, \tag{4.6}$$

starting at about 6 ns and increasing in steps of approximately 0.5 ns, and to evaluate the given results for the parameters. Because of the criteria given for the parameter, $r_0 < 0.4$, $y_0 \approx 0$ and $\theta > 0$, it was possible to exclude some of the tried ranges and to find the best fit under these circumstances.

For the pure GFP-water mixture, the results for θ are close to the expectation (see table 4.4) but for the 20 % glycerol mixture, the problematic becomes clear, because θ matches with the value from 4.4 but in both measurements, r_0 is greater than 0.4. This problem extended for higher concentrations, and when the parameters showed allowed values, the rotational correlation time was far away from the theoretical considerations, e. g. for higher concentrations lower than for 0 %, which means that the GFP rotates faster when the viscosity increases. This however, is illogical and does not make sense.
Due to this outcome, it is convincing to look at the theoretical expectations first, and to discuss the measured data afterwards again.

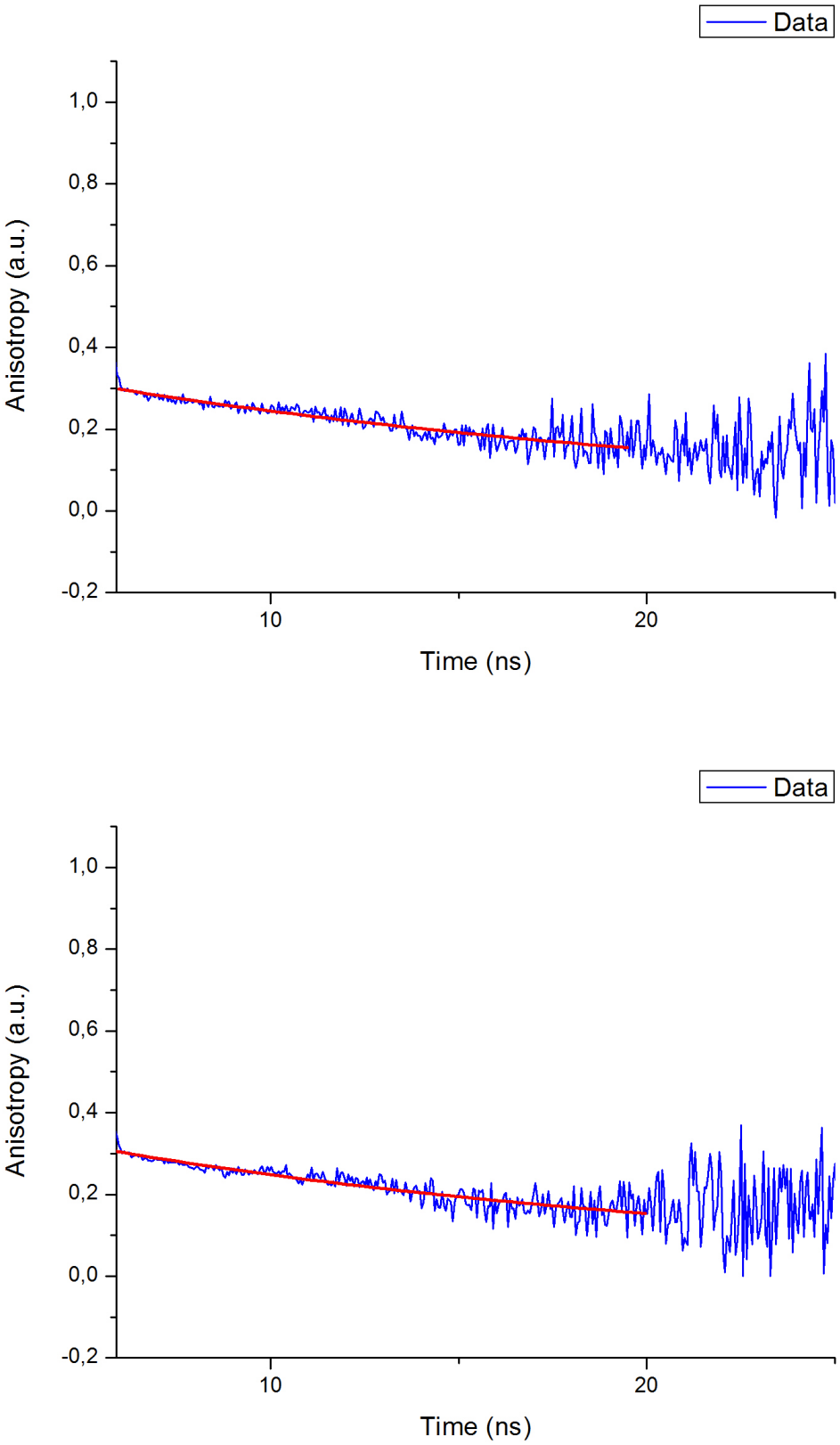

FIGURE 4.7: Anisotropy decay for 0 %, first measurement at the top with the parameters $r_0 = 0.39 \pm 0.06$, $\theta = 20.1 \pm 7.7$ ns and $R^2 = 0.77$ and second measurement at the bottom with the parameters $r_0 = 0.39 \pm 0.04$, $\theta = 18.3 \pm 5.7$ ns and $R^2 = 0.79$

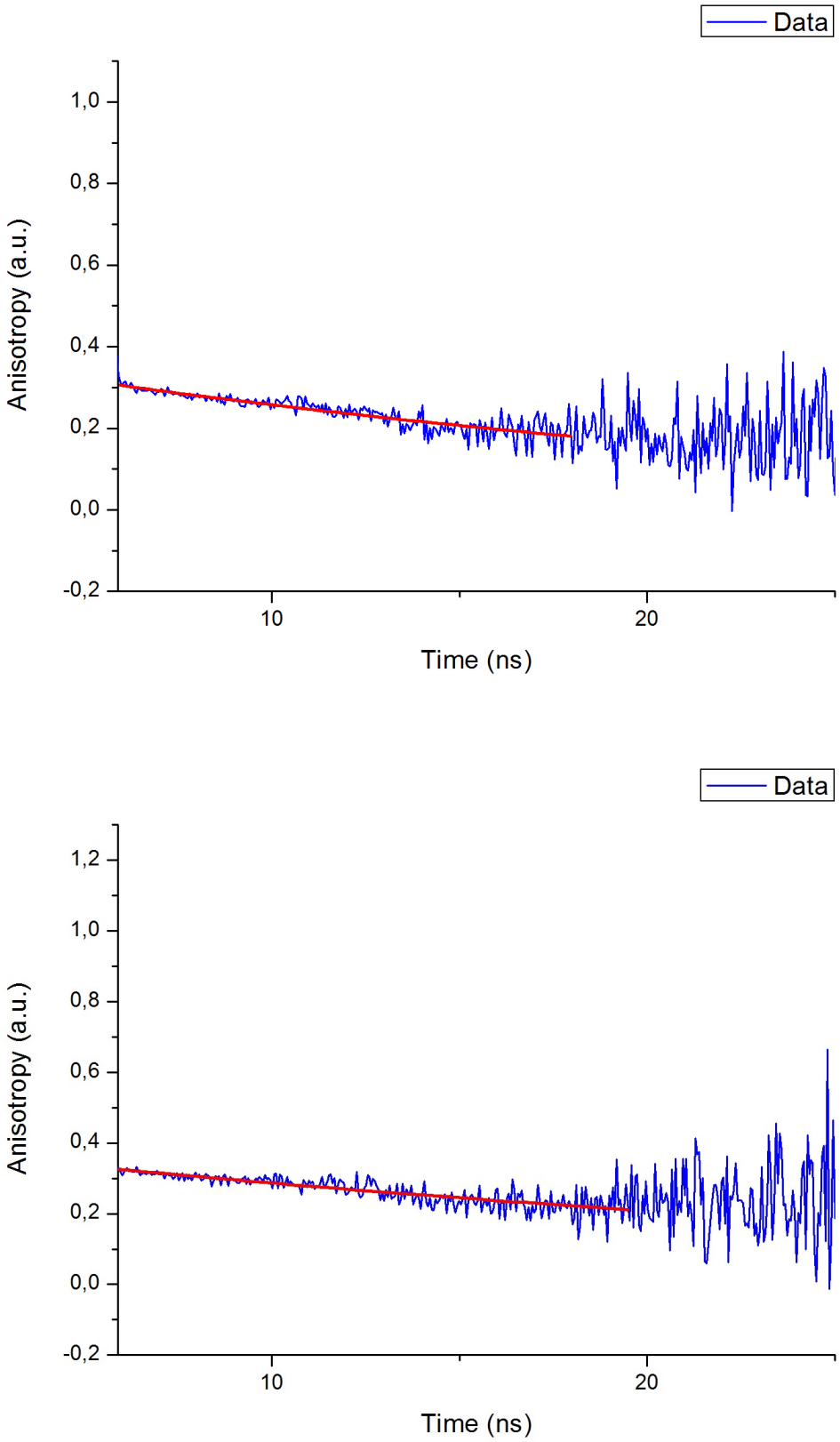

FIGURE 4.8: Anisotropy decay for 20 %, first measurement at the top with the parameters $r_0 = 0.5 \pm 0.2$, $\theta = 30.1 \pm 20.2$ ns and $R^2 = 0.77$ and second measurement at the bottom with the parameters $r_0 = 0.4 \pm 0.3$, $\theta = 36.7 \pm 34.5$ ns and $R^2 = 0.64$

TABLE 4.3: Rotational correlation time θ_{Stokes} and $\theta_{cylinder}$ of GFP for the studied concentrations of glycerol, viscosity calculated by [23]

Concentration [%]	Dynamic viscosity η [Ns/m^3]	θ_{Stokes} [ns]	$\theta_{cylinder}$ [ns]
0	0.0010	23	4.7
20	0.0020	46	9.3
39	0.0046	106	21
50	0.0084	194	39
60	0.016	373	75
68	0.030	689	139
78	0.074	1724	349
82	0.11	2629	532

4.1.4 Theoretical Expectation

The rotational correlation time is the magnitude of interest in the anisotropy measurement experiments. Its expression is given by [5] [1]

$$\theta = \frac{\eta V}{k_B T}. \tag{4.7}$$

k_B is the Boltzmann constant, η the dynamic viscosity of the water-glycerol solution, T the ambient temperature and V the volume of the rotating unit, in this case the GFP. The dynamic viscosity can be obtained by introducing actual water and glycerol quantities in the calculation application [23] which is based on the work [24]. Assuming that the temperature during the experimental sessions was $T = 293.15\,\text{K}$, there is only the GFP volume missing.

Based on the Stokes-Einstein-Debye equation The first method to express the volume of GFP involves the rotational diffusion coefficient[25]

$$D = \frac{k_B T}{8\pi\eta r_h^3} \tag{4.8}$$

r_h describes the hydrodynamic radius (Stokes radius) of the protein, in the way that

$$\theta_{Stokes} = \frac{1}{6D} = \frac{4\pi\eta r_h^3}{3k_B T}. \tag{4.9}$$

Obviously, this expression for θ assumes a spherical shape for the protein. It can be considered that the Stokes radius of GFP is 2.82 nm[26], and the resulting volume is $V_{Stokes} = 9.39 \times 10^{-26}\,\text{m}^3$. The corresponding rotational correlation times can be found in table 4.3.

TABLE 4.4: Rotational correlation time θ_{exp} and θ_{ideal} of GFP for the studied concentrations of glycerol, viscosity calculated by [23]

Concentration [%]	Dynamic viscosity η [Ns/m^3]	θ_{exp} [ns]	θ_{ideal} [ns]
0	0.0010	**19**	**20**
20	0.0020	39	40
39	0.0046	88	91
50	0.0084	166	166
60	0.016	321	320
68	0.030	594	591
78	0.074	1451	1478
82	0.11	2220	2254

Considering a cylindric shape Knowing that the GFP actually presents a barrel shape, resulting from previous studies, the volume corresponds to a cylinder with a diameter of 2.4 nm and a length of 4.2 nm [27]. In this case, however, the volume is $V_{cylinder} = 1.9 \times 10^{-26}\,\mathrm{m}^3$. The values of the rotational correlation time $\theta_{cylinder}$ for this volume and the varying viscosity are shown in table 4.3.

Based on the results for pure water-GFP mixture The last method to find a theoretical value of the rotational correlation time for comparison, is to assume that the first measurement, so the pure water-GFP probe without adding glycerol, is reliable. Making use of this result and the viscosity of the pure mixture, the volume V_0 can be determined. Since this value is universally valid, inserting V_0 in 4.7 and varying the viscosity leads to the expectations for θ, called θ_{exp}.
Relying on previous studies [28] which postulate an ideal rotational correlation time of GFP in water about 20 ns and repeating the procedure as before, the ideal values θ_{ideal} for each concentration can be obtained. In table 4.4 the results for θ_{exp} and θ_{ideal} are summed up. The first value of 0 % glycerol is the average of the results obtained in the two measurements from 4.7.

The first value for $\theta_{exp} = 19$ ns 4.7 deviates with 3.9 % from the θ_{ideal}. The average taken from 4.8, $\theta = 33$ ns, already presents a greater deviation, 13 % from θ_{exp} and 15 % from θ_{ideal}. As only these two results serve for evaluating the shape models, it can be said that the approximation of a sphere is much closer to the measured values than the cylindric shape. The low values for the cylinder may result in the fact that it was not considered that water molecules may be attached to the protein, enlarging the effective volume

that participates in the rotation. The assumption of a spherical shape gives slightly higher rotational correlation times and knowing the real shape of the GFP, it only represents an approximation. Without expecting great accuracy, this model turns out to be better than merely considering a cylinder and ignoring its aqueous environment.

At the beginning of the paragraph, it was indicated that the plan of fitting the data and obtaining values for the rotational correlation time does not work out. However, to make an evaluation of the data possible, the theoretical values θ_{exp} from table 4.4 were plotted in the corresponding data graphic, adjusting the initial anisotropy in the way that the curve coincides best with the data. The reason why θ_{exp} was used instead of θ_{ideal} is that θ_{exp} already includes the specific error.

Another idea based on this procedure is to estimate the fitting range better, and to choose the new limit where the curve does not coincide with the data anymore, albeit the problematic of inconsistent results could not be eliminated.

The resulting graphics for every concentration are combined in the figures 4.9 to 4.15 to observe the development. Apparently, in every case, the ideal curve is similar to the data for the beginning time ranges, but later on, the theoretic curve separates from the measurements, which decay faster. Therefore, the rotational correlation time is always smaller than the expectation. A reason for the difference between expectation and results could also be the increasing scattering at higher concentrations, because every time a photon is scattered, the polarization changes [1]. Also the scattering of the excitation light in the probe cannot be avoided, so the considerations about the change of polarization and therefore also of the anisotropy, are valid for both, excitation and emission radiation.

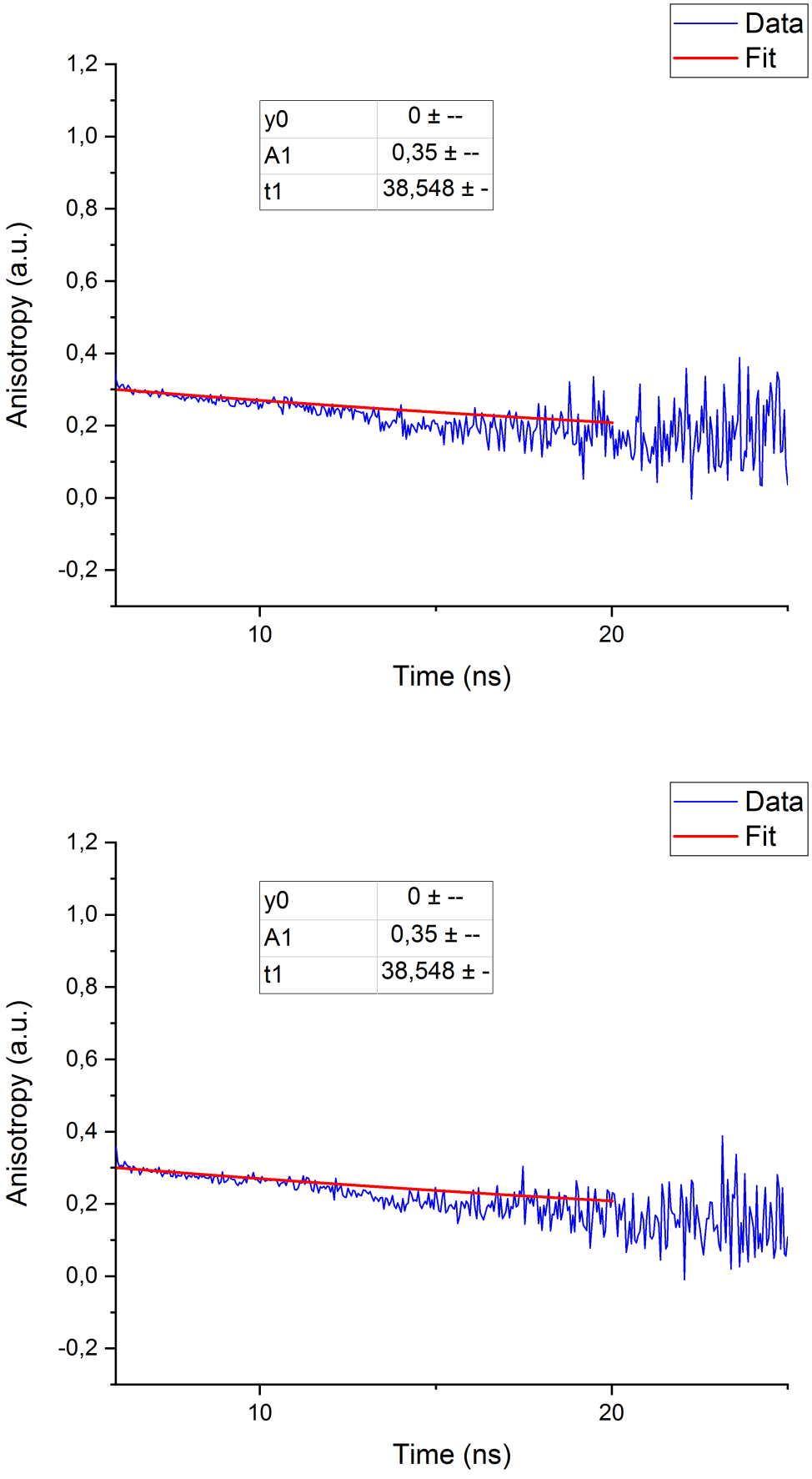

FIGURE 4.9: Anisotropy decay results for 20 % concentration with the ideal curve fit from table 4.4 column θ_{exp}, first measurement at the top, second measurement at the bottom

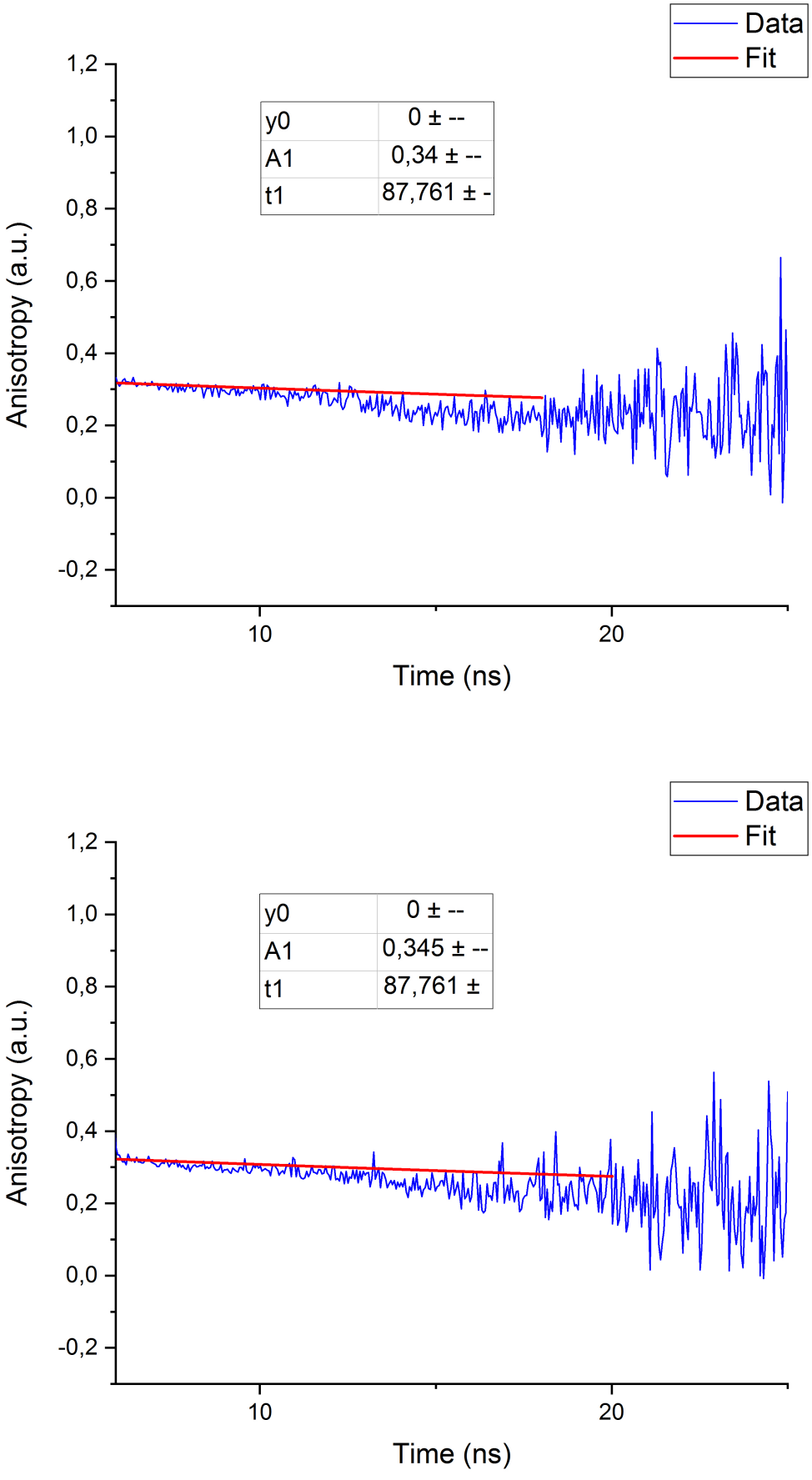

FIGURE 4.10: Anisotropy decay results for 39 % concentration with the ideal curve fit from table 4.4 column θ_{exp}, first measurement at the top, second measurement at the bottom

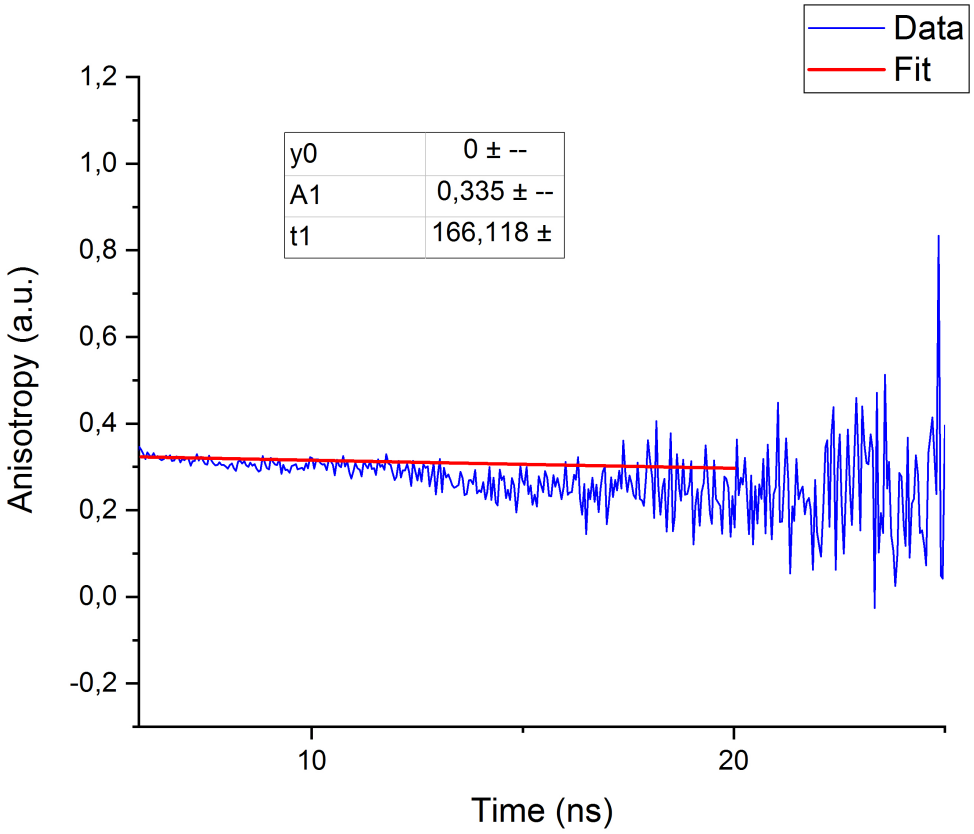

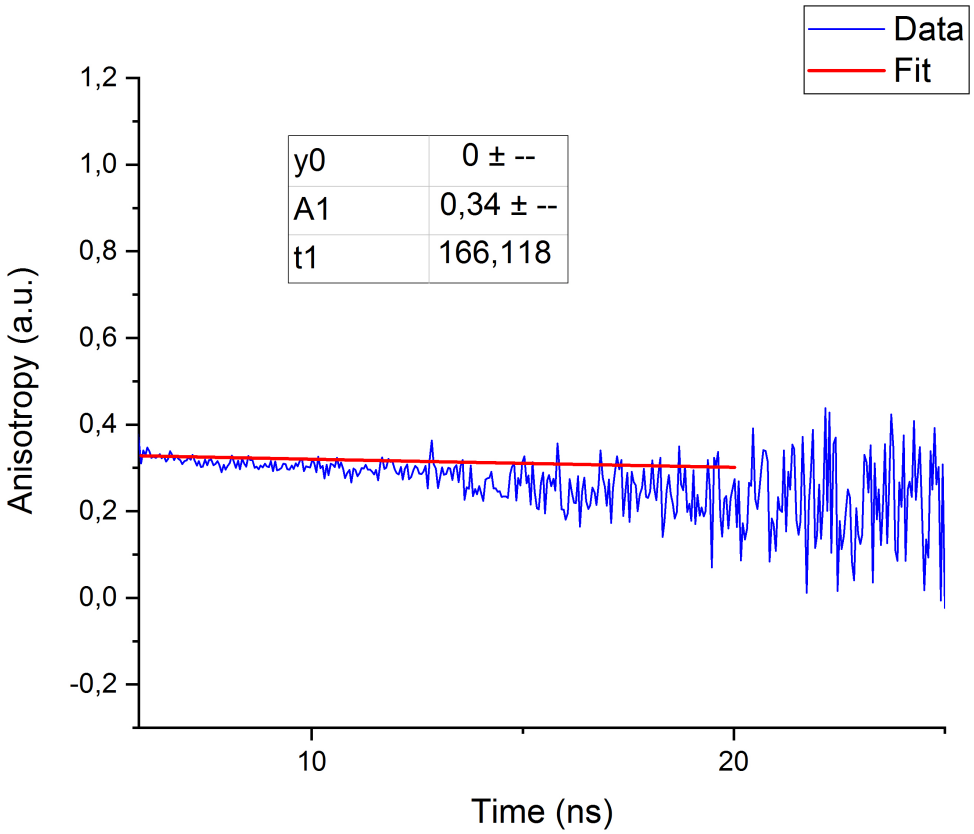

FIGURE 4.11: Anisotropy decay results for 50 % concentration with the ideal curve fit from table 4.4 column θ_{exp}, first measurement at the top, second measurement at the bottom

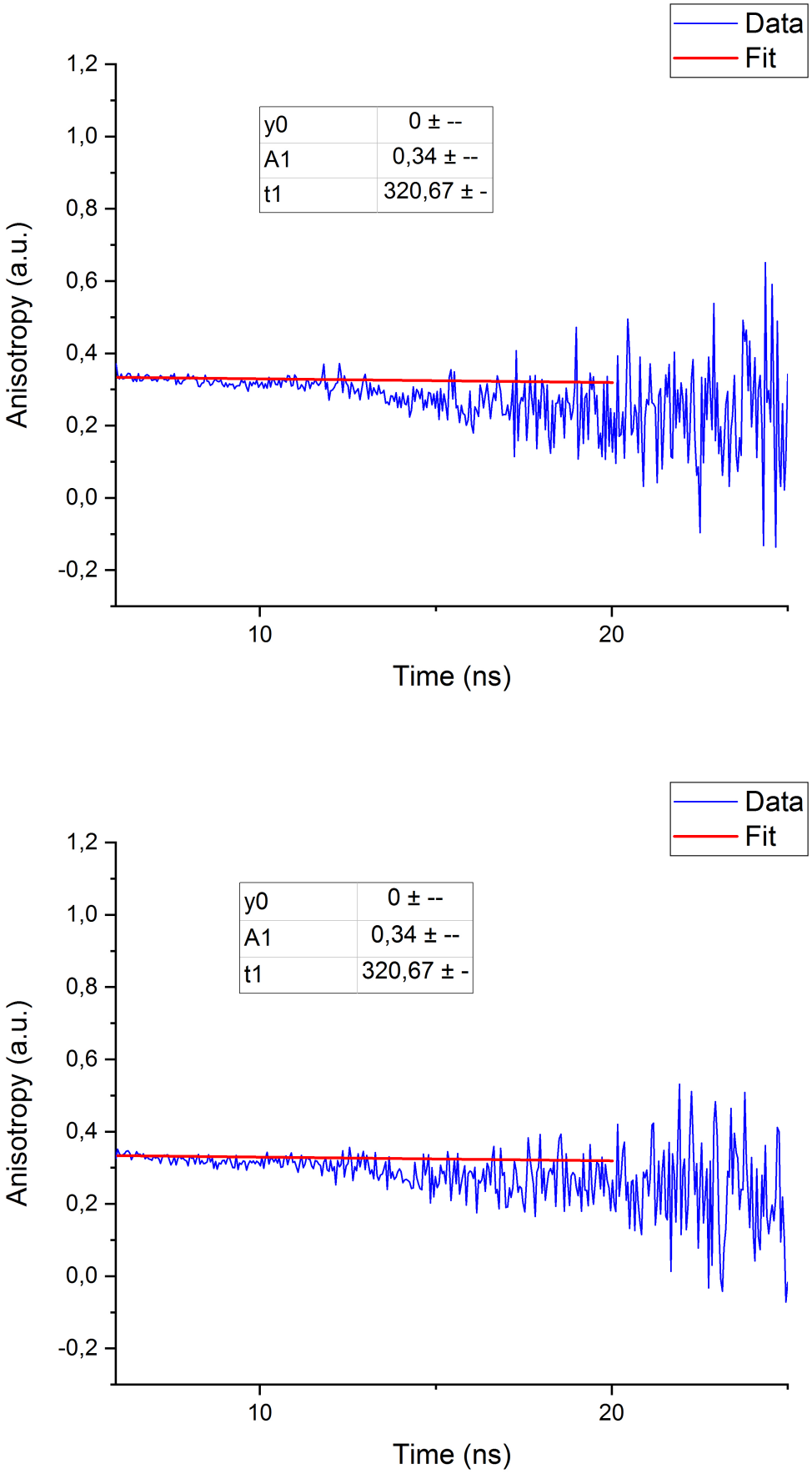

FIGURE 4.12: Anisotropy decay results for 60 % concentration with the ideal curve fit from table 4.4 column θ_{exp}, first measurement at the top, second measurement at the bottom

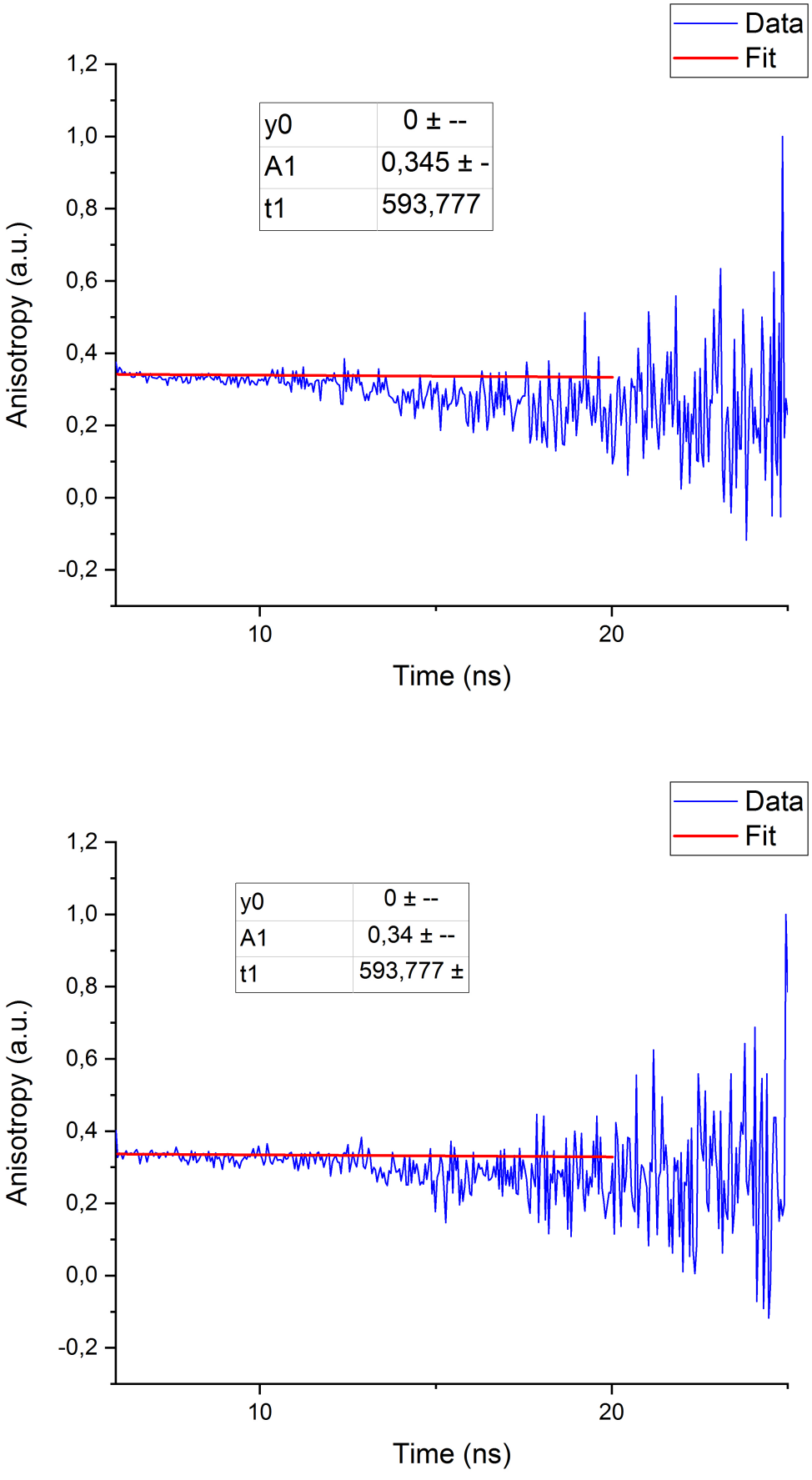

FIGURE 4.13: Anisotropy decay results for 68 % concentration with the ideal curve fit from table 4.4 column θ_{exp}, first measurement at the top, second measurement at the bottom

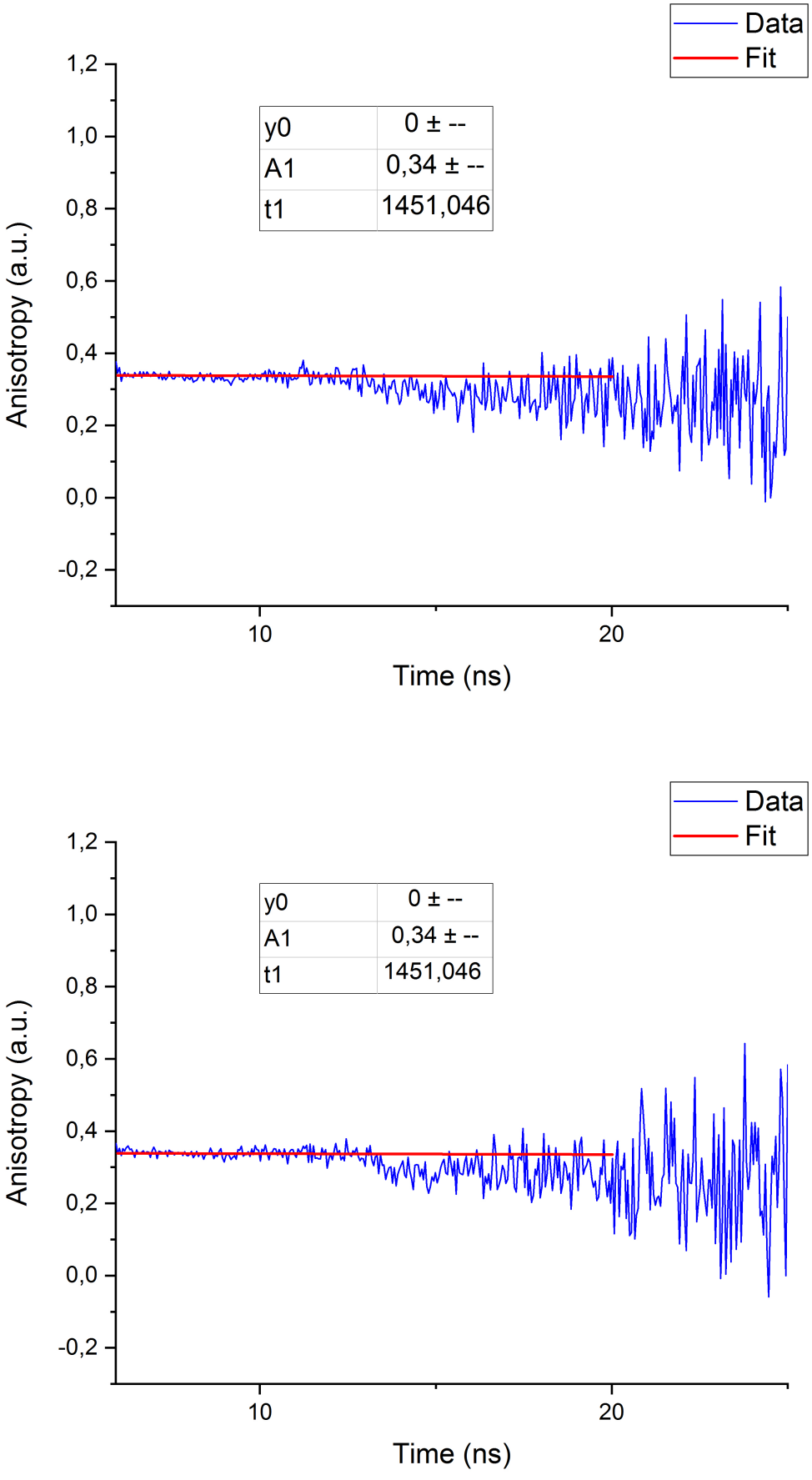

FIGURE 4.14: Anisotropy decay results for 78 % concentration with the ideal curve fit from table 4.4 column θ_{exp}, first measurement at the top, second measurement at the bottom

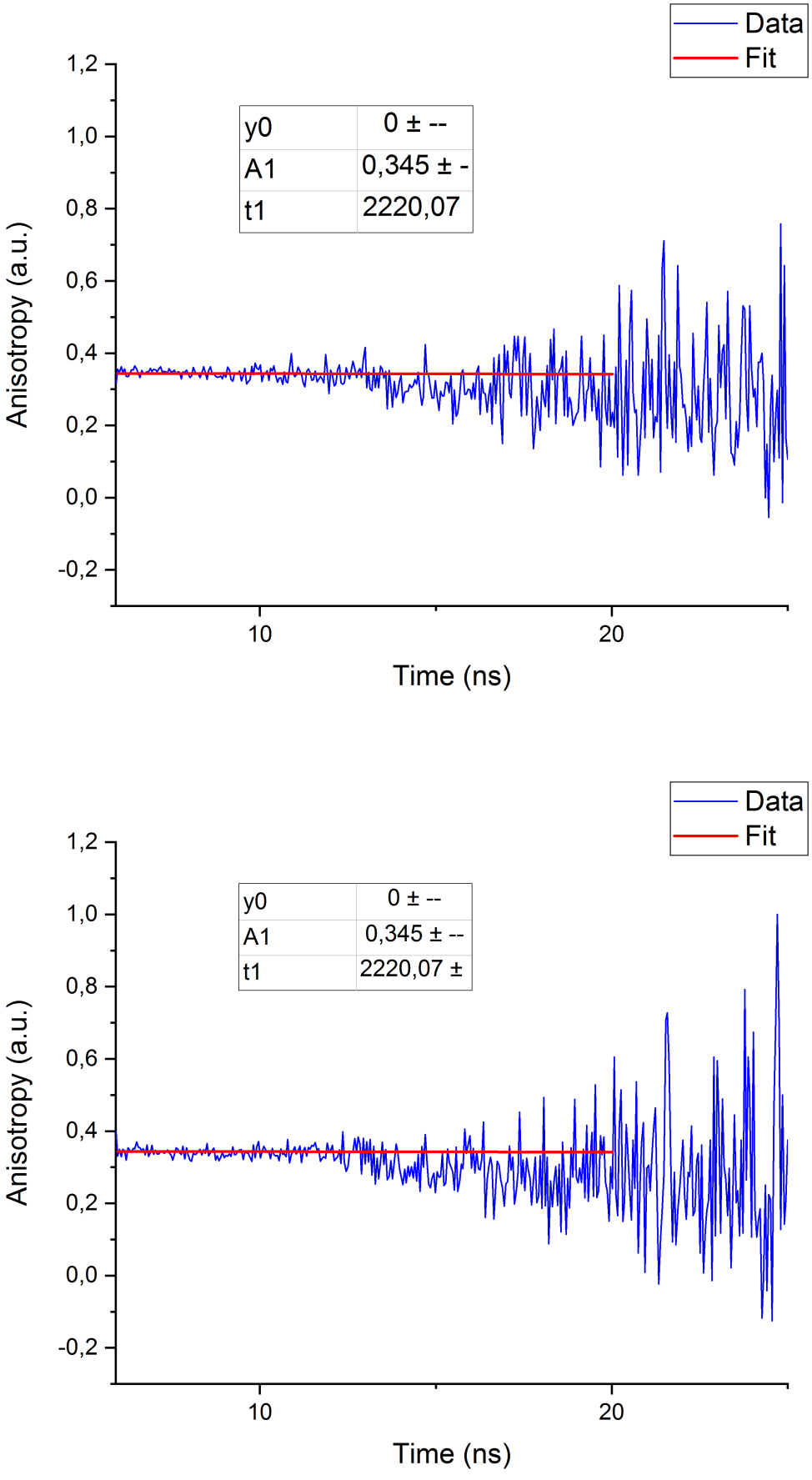

FIGURE 4.15: Anisotropy decay results for 82 % concentration with the ideal curve fit from table 4.4 column θ_{exp}, first measurement at the top, second measurement at the bottom

Chapter 5

Conclusion

Resumen

A modo de conclusión, se incide en el éxito en la medición del espectro de emisión y el significado físico del mismo. Además, se clasifica el tipo de la GFP utilizada a partir de los resultados obtenidos. Por otro lado, el comportamiento del tiempo de vida y la disminución del valor de τ con el aumento de la concentración de glicerina, permiten concluir que una medida de τ también sirve para caracterizar el medio entorno de la proteína, igual que las medidas de anisotropía. Así, para mejorar los resultados de la desintegración de la anisotropía se propone una disminución de la temperatura que permita cambiar la viscosidad de la mezcla en lugar de aumentar la concentración, con el fin de minimizar el error. Finalmente, en relación a los modelos de la forma del GFP, se presenta la posibilidad de suponer la forma de un elipsoide para obtener una aproximación mejor.

Starting the analysis with the emission spectrum, it can be concluded that the spectrum is not changed by the environmental viscosity, including that the involved energy levels and their transition probabilities stay the same during the increase of glycerol. Also the detected value for the peak only shows a relative deviation of 0.20 % from the expected theoretical value. Knowing the excitation wavelength, in this case, a laser of 470 nm, and the emission peak, and making use of the table from [7] on page 519, the used GFP can be classified as a wild type GFP and no mutation.
Unlike the emission spectrum, the lifetime decay and the obtained lifetime value τ is altered by the concentration of glycerol. Precisely, the electrons remain less time in the excited state at high concentrations, so they return faster to the ground state than it can be observed in lower concentrations. This result is similar to a previous study [22], which also works with GFP and increasing glycerol amounts. The Strickler Berg formula, which is relating the refractive index with the fluorescence lifetime, indicates that a measurement

of τ (fluorescence lifetime imaging microscopy FLIM) can be used to study the environment of the fluorescent protein and to find out the refractive index of the surrounding medium.
The second measuring session of the anisotropy, however, did not turn out as expected either. Like already mentioned, it is suspected that scattering and other mechanisms that influence the fluorescence (as described in 1.1) and the anisotropy, such as reabsorption of emitted photons [1] by the GFP, are responsible for the results.
Furthermore, it may be an option to leave the concentration fixed, using 0.88 ml water-GFP and 0.22 ml for a mixture of 20 % glycerol, and increasing the temperature in the sample chamber. As the viscosity depends on the temperature, the same mixture at around $-48\,^{\circ}\mathrm{C}$ has the same viscosity like a mixture of 82 % glycerol [23]. The freezing point has to be taken into account, so the initial mixture has to be chosen in order to avoid problems with freezing. With this technique, errors caused by the repeated mixing process when glycerol is added, like the loss of glycerol or water-GFP, can be avoided. Also a new adjustment of the probe in the laser beam is not necessary and the connected errors can be minimized.
Relating to the shape models, it may be convincing to consider another shape, like an ellipsoid [1] instead of a sphere because it appears closer to a barrel than a sphere. The shape of the curves indicate that no segmental rotation exists. This fact agrees with the expectation as a barrel has no additional parts that can rotate independently, producing a distinct anisotropy decay.

Appendix A

Additional graphics

A.1 Lifetime Decay

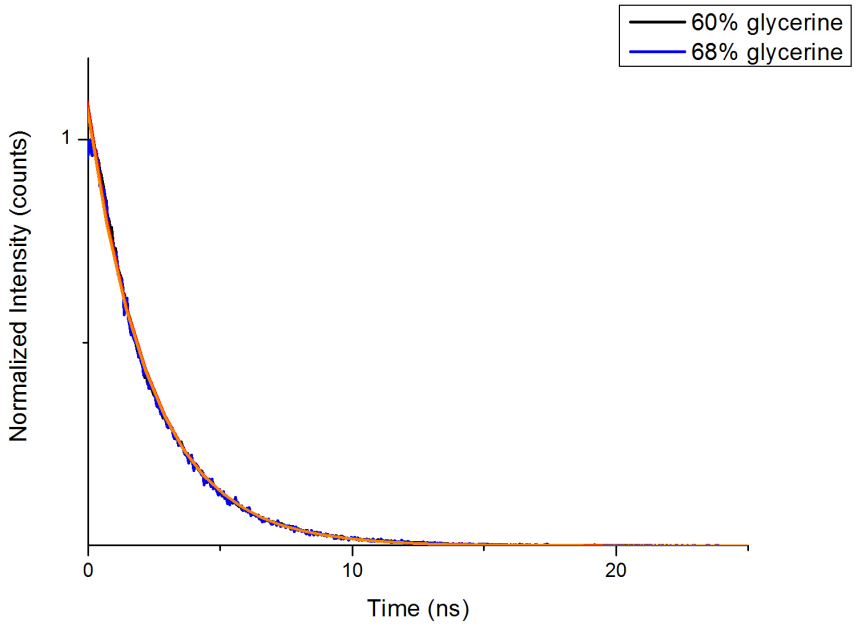

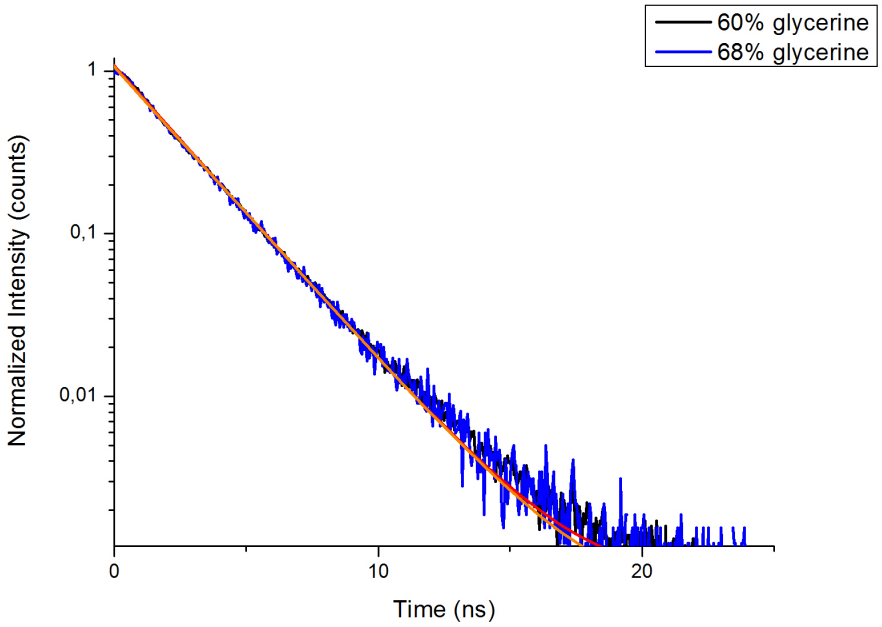

FIGURE A.1: Fluorescence lifetime decay of 60 % and 68 % glycerol solvents. Normal scale (at the top), logarithmic scale (at the bottom). The lifetime values are $\tau_{60} = 2.401(7)$ ns and $\tau_{68} = 2.417(8)$ ns, coefficients of determination $R^2_{60} \approx 1$ and $R^2_{68} \approx 1$

Bibliography

[1] J. R. Lakowicz. *Principles of Fluorescence Spectroscopy*. 3rd ed. Springer, 2006.

[2] G. H. Patterson et al. "Use of the Green Fluorescent Protein and Its Mutants in Quantitative Fluorescence Microscopy". In: *Biophysical Journal* (1997).

[3] A. Volkmer et al. "One- and Two-Photon Excited Fluorescence Lifetimes and Anisotropy Decays of Green Fluorescent Proteins". In: *Biophysical Journal* (2000).

[4] S. V. Koushik et al. "Energy migration alters the fluorescence lifetime of Cerulean: implications for fluorescence lifetime imaging Forster resonance energy transfer measurements". In: *NIH Public Access* (2008).

[5] R. Swaminathan et al. "Photobleaching Recovery and Anisotropy Decay of Green Fluorescent Protein GFP-S65T in Solution and Cells: Cytoplasmic Viscosity Probed by Green Fluorescent Protein Translational and Rotational Diffusion". In: *Biophysical Journal* (1997).

[6] Chemistry and Light. *Fluorescence*. 2018. URL: http://www.chemistryandlight.eu/index.php/fluorescence/.

[7] R. Y. Tsien. "The green flourescent protein". In: *Annual reviews* (1998), p. 36.

[8] M. Ehrenberg. "The green flourescent protein: discovery, expression and development". In: *by the Royal Swedish Academy of Science* (2008), p. 18.

[9] Inc. BioTek Instruments. *Excitation and Emission of Green Fluorescent Proteins*. 2018.

[10] T. King et al. *Green Flourescent Protein*. University of Bristol. URL: http://www.chm.bris.ac.uk/motm/GFP/GFPh.htm.

[11] R. Heim et al. "Engineering green fluorescent protein for improved brightness, longer wavelengths and fluorescence resonance energy transfer". In: *Current Biology* (1996). URL: http://www.sciencedirect.com/science/article/pii/S0960982202004505.

[12] B. Herman et al. *Fluorophores for Confocal Microscopy*. URL: https://www.olympus-lifescience.com/en/microscope-resource/primer/techniques/confocal/fluorophoresintro/.

[13] B. Manicassamy et al. "Analysis of in vivo dynamics of influenza virus infection in mice using a GFP reporter virus". In: *Proceedings of the National Academy of Science of the United States of America (PNAS)* (2010).

[14] E. Terpetschnig et al. *Fluorescence Lifetime (FLT)*. URL: http://www.iss.com/resources/research/technical_notes/K2CH_FLT.html.

[15] J. A. Levitt et al. *Fluorescence lifetime imaging microscopy*. 2009. URL: https://eic.rsc.org/feature/fluorescence-lifetime-imaging-microscopy/2020147.article.

[16] T. J. Zielinski et al. *Quantum States of Atoms and Molecules*. 2017. URL: https://chem.libretexts.org/Textbook_Maps/Physical_and_Theoretical_Chemistry_Textbook_Maps/Book%3A_Quantum_States_of_Atoms_and_Molecules_(Zielinksi_et_al.)/04._Electronic_Spectroscopy_of_Cyanine_Dyes/4.04%3A_The_Transition_Dipole_Moment_and_Spectroscopic_Selection_Rules.

[17] Azo Materials. *LifeSpec II – High-Performance Fluorescence Spectrometer*. 2013. URL: https://www.azom.com/article.aspx?ArticleID=9293.

[18] PicoQuant. *Fluorescence Lifetime Imaging (FLIM)*. URL: https://www.picoquant.com/applications/category/life-science/fluorescence-lifetime-imaging-flim.

[19] K. Suhling et al. "Imaging the environment of green fluorescent protein." In: *Biophysical journal* 83 6 (2002), pp. 3589–95.

[20] S. J. Strickler et al. *Citation Classic: Relationship between absorption intensity and fluorescence lifetime of molecules*. Chem. Phys. 37:814-22. 1962. URL: http://garfield.library.upenn.edu/classics1981/A1981MT33200001.pdf.

[21] Multidisciplinary Engineering. *Refractive index glycerin water*. URL: http://edge.rit.edu/edge/P13051/public/Research%20Notes/refractive%20index%20glycerin%20water.pdf.

[22] L. F. Hoyt. "Determination of refractive index of glycerols by the immersion refractometer". In: *Oil and Soap* 10.3 (), p. 43. DOI: 10.1007/BF02639078. eprint: https://onlinelibrary.wiley.com/doi/pdf/10.1007/BF02639078. URL: https://onlinelibrary.wiley.com/doi/abs/10.1007/BF02639078.

[23] *Calculate density and viscosity of glycerol water mixtures*. 2018. URL: http://www.met.reading.ac.uk/~sws04cdw/viscosity_calc.html.

[24] N.-S. Cheng. "Formula for the Viscosity of a Glycerol Water Mixture". In: *Industrial & Engineering Chemistry Research* 47.9 (2008), pp. 3285–3288. URL: https://doi.org/10.1021/ie071349z.

[25] A. Loman et al. "Measuring rotational diffusion of macromolecules by fluorescence correlation spectroscopy". In: 9 (May 2010), pp. 627–36.

[26] *Stokes radius of Green Fluorescent Protein*. URL: http://bionumbers.hms.harvard.edu/bionumber.aspx?id=104396.

[27] M. A. Hink et al. "Structural Dynamics of Green Fluorescent Protein Alone and Fused with a Single Chain Fv Protein". In: 275 (July 2000), pp. 17556–60.

[28] A. Partikian et al. "Rapid Diffusion of Green Fluorescent Protein in the Mitochondrial Matrix". In: *The Journal of Cell Biology* 140.4 (1998), pp. 821–829. ISSN: 0021-9525. DOI: 10.1083/jcb.140.4.821. eprint: http://jcb.rupress.org/content/140/4/821.full.pdf. URL: http://jcb.rupress.org/content/140/4/821.